Legendrian and transverse knots in the light of Heegaard Floer Homology

Vera Vértesi

PhD Thesis submitted to

Eötvös Loránd University
Institute of Mathematics

Doctoral School	:	Mathematics
Director	:	Miklós Laczkovich member of the Hungarian Academy of Sciences
Doctoral Program	:	Pure Mathematics
Director	:	András Szűcs corresponding member of the Hungarian Academy of Sciences
Supervisors	:	András I. Stipsicz (Rényi Institute) Doctor of Sciences
		Csaba Szabó Doctor of Sciences

Budapest
2009

Acknowledgement

I am deeply grateful to both of my advisors; Csaba Szabó, with whom I first experienced the joy of doing research and András Stipsicz, who showed me some insights of low dimensional topology.

It is a pleasure to acknowledge several organizations and institutions which facilitated or sponsored my research. I was supported by the "Magyar Állami Eötvös Ösztöndíj" and by NSF grant number FRG-0244663 and OTKA 67867, 67870 and 49449. These supports gave me the opportunity to spend two semesters at Columbia University and three month at Georgia Institute of Technology. The exceptionally nice and vibrating community of the Maths department at Columbia was very inspiring; It was a pleasure to participate at the "Informal Graduate Seminar". I take this opportunity to thank Peter Ozsváth and the people from the department and the graduate students of Columbia for their hospitality. During the whole period of my visit at Columbia I had regular meetings with András Stipsicz. Most of the results of this dissertation resulted from these conversations. I owe him a lot for his encouraging and help. Although the work I did at GeorgiaTech will not appear in this thesis, the research experience with John Etnyre was fun and also very useful I am especially grateful his patience. I would also like to thank Ko Honda and Paolo Ghiggini for helpful discussions.

I am indebted to László Surányi and Lajos Pósa who taught and advised me during my high school and undergraduate years, and shaped my mathematical viewpoint. I am also grateful to Róbert Sződi.

Finally, I would like to thank my family for their support. This dissertation is dedicated to them.

Contents

1. Introduction

Although contact geometry was born in the late 19th century in the work of Sophus Lie, its 3–dimensional version has just recently started to develop rapidly, with the discovery of convex surface theory and by recognizing its role in other parts of topology. For example Property P for knots —a possible first step for resolving the Poincaré conjecture— was proved using contact 3–manifolds (Kronheimer-Mrowka [29]). Also, the fact that Heegaard Floer homology determines the Seifert genus of a knot was first proved with the help of contact 3–manifolds (Ozsváth-Szabó [38]). Being the natural boundaries of Stein domains, the use of contact 3–manifolds resulted in a topological description of Stein-manifolds. A contact structure on an oriented 3–manifold is a totally non-integrable plane field. In other words it is a plane distribution that is not everywhere tangent to any open embedded surface. Any 3–manifold admits a contact structure (Martinet [33]). It is more subtle to understand the set of all different contact structures on a given 3–manifold. One way to understand them is by examining lower dimension submanifolds that respect the structure in some way. The 1–dimensional such submanifolds are Legendrian and transverse knots.

Invariants that are fruitfully used to distinguish contact structures and Legendrian and transverse knots come from Heegaard Floer homology. Heegaard Floer homologies, (Ozsváth-Szabó, [40, 41, 43]) the recently-discovered invariants for 3- and 4-manifolds, come from an application of Lagrangian Floer homology to spaces associated to Heegaard diagrams. Although this theory is conjecturally isomorphic to Seiberg-Witten theory, it is more topological and combinatorial in its flavor and thus easier to work with in certain contexts. These homologies admit generalizations and refinements for knots (Ozsváth-Szabó [39] and Rasmussen [46]) and links (Ozsváth-Szabó [44]) in 3–manifolds and for non-closed 3–manifolds with certain boundary conditions (Juhász [26]), called sutured Floer homology. The tools used to define the link-version were later applied to define a completely combinatorial version of knot Floer homology in the 3–sphere. In Heegaard Floer homology contact invariants were defined for contact 3–manifolds without (Ozsváth-Szabó [42]) or with (Honda-Kazez-Matic [24]) boundary. These invariants had many applications, the most recent is a new proof for the fact that a contact 3–manifold having Giroux torsion cannot be Stein-fillable (Ghiggini-Honda-Van Horn-Morris [20]).

There are two ways for a one dimensional submanifold to respects the contact structure. Its tangents can entirely lie in the plane distribution, in which case the knot is called Legendrian knot, or if the tangents are transverse to the planes, then the knot is called a transverse knot. The question underlying contact knot theory is simple: when are two Legendrian or transferse knots the same, i.e., isotopic through Legendrian or transversal knots? This question was first explicitly stated in [1] and also appears in Kirby's problem list [28].

Legendrian and transverse knot theory has been shaped by advances in convex surface theory [16] (showing that different looking objects are actually equivalent) and by the introduction of various invariants of these knots — proving that different looking objects are, in fact, different. Examples of such invariants are provided by Chekanov's differential graded algebras and contact homology [4, 8]. More recently, Heegaard Floer homology provided various sets of invariants: for knots in the standard contact 3–sphere the combinatorial construction of knot Floer homology through grid diagrams [35, 45], for null–homologous knots in general contact 3–manifolds the Legendrian invariant of [30] and for general Legendrian knots the sutured invariant of the knot complement [24]. In this dissertation we study these invariants to get a better understanding of Legendrian and transverse knots.

This dissertation is organized as follows. In Section 2 we give a brief overview of the different versions of Heegaard Floer homologies we will use. Section 3 is an introduction to contact 3–manifolds, including basic definitions and facts about Legendrian and transverse knots, convex surface theory, open book decompositions, partial open book decompositions and bypass attachments. Then in Section 4 we connect the previous two Sections and define invariants for Legendrian and transverse knots in Heegaard Floer homology, in Section 5 we prove a relation between two of the invariants defined. Using this relation we derive new properties of the Legendrian invariant. In Section 6 we obtain a connected-sum formula for the combinatorial invariant and as a corollary we give a construction of infinitely many transversely non-simple knot types.

2. Heegaard Floer theories

Heegaard Floer homologies are invariants for 3–manifolds and knots in 3–manifolds. The original theories for closed 3–manifolds $\widehat{\mathrm{HF}}$, HF^-, HF^+ and $\mathrm{HF}_{\mathrm{red}}$ were defined by Ozsváth and Szabó, and then were generalized for null-homologous knots ($\widehat{\mathrm{HFK}}$ and HFK^-) by Ozsváth and Szabó [44] and independently by Rasmussen [46]. A related theory SFH was introduced by Juhász [26] for 3–manifolds with certain boundary conditions. All these theories arise from Lagrangian Floer theories associated to a Heegaard decompositions of the 3–manifold. In the sequel we will give a brief description for these theories. For a more complete treatment the reader is referred to [41, 40, 43, 39, 26]. In Subsection 2.1 and 2.2 we give the preliminaries that are necessary for the definition of Heegaard Floer homologies, and in Subsection 2.3 we will describe the original Heegaard Floer theories. In Subsection 2.4 we define the refinement of Heegaard Floer homologies for knots, then in Subsection 2.5 we introduce multiply pointed Heegaard diagrams and generalize the previous theories to these settings. Multiply pointed Heegaard diagrams are the major tools to define a combinatorial version of knot Floer homology in the 3–sphere, this will be described in Subsection 2.6. Then Subsection 2.7 deals with sutured Floer homology which is a common generalization of the $\widehat{\ }$-theories.

2.1. **Heegaard decompositions and Heegaard diagrams.** A *genus g handlebody* U is a 3–manifold with boundary diffeomorphic to the neighborhood of a bouquet of g circles. The boundary of a genus g handlebody is a surface Σ of genus g. A Heegaard decomposition of a 3–manifold Y is a decomposition of Y to two handlebodies: $Y = U_\alpha \cup_\Sigma U_\beta$. Here Σ is oriented as the boundary of U_α. For example S^3 has a Heegaard decomposition to two 3–balls. For another example let $S^3 = S^3_1 = \{|(z_1, z_2)| = 1\} \subset \mathbb{C}^2$, then $U_\alpha = \{|z_1| \leq |z_2|\} \cap S^3$ and $U_\beta = \{|z_2| \leq |z_1|\} \cap S^3$ gives a Heegaard decomposition of genus 1, the gluing map $T^2 = \partial U_\alpha \to T^2 = \partial U_\beta$ brings the meridian of ∂U_α to a longitude of ∂U_β. 3–manifolds with genus 1 Heegaard splittings are called lens spaces. Any 3–manifold admits a Heegaard decomposition. Indeed, smooth manifolds admit triangulations, and the neighborhood of the 1–skeleton and its complement (which is a neighborhood of the dual 1-skeleton) provides a Heegaard decomposition. The introduction of a new edge in the triangulation increases the genus of the Heegaard decomposition by one, this is called *stabilization* of the Heegaard decomposition. Heegaard decompositions can be described by two sets of curves on Σ as follows. A properly

embedded disc D in a handlebody U whose boundary γ is homologically nontrivial on Σ is called a *compressing disc*. Choose g disjoint compressing discs in U that cut U up to a ball, and denote their boundaries by $\boldsymbol{\gamma} = \{\gamma_1, \dots, \gamma_g\}$. The curves $\{\gamma_1, \dots, \gamma_g\}$ are disjoint, and are independent in $H_1(\Sigma; \mathbb{Z})$. Conversely a set of disjoint curves $\{\gamma_1, \dots, \gamma_g\}$ on Σ that are independent in $H_1(\Sigma; \mathbb{Z})$ describe a handlebody; attaching thickened discs to the thickened surface Σ along the $\boldsymbol{\gamma}$–curves, we obtain a 3–manifold with boundary $\Sigma \cup S^2$, and there is a unique way to fill in the sphere with a ball. Note that this g-tuple of boundaries of compressing discs is not unique; if we isotope the $\boldsymbol{\gamma}$–curves they will still describe the same handlebody. The handlebody also remains unchanged if we change the set $\boldsymbol{\gamma} = \{\gamma_1, \gamma_2 \dots, \gamma_g\}$ to $\boldsymbol{\gamma}' = \{\gamma_1 + \gamma_2, \gamma_2, \dots, \gamma_g\}$, where $\gamma_1 + \gamma_2$ is a curve that bounds a pair of pants with γ_1 and γ_2 disjoint from $\{\gamma_3, \dots, \gamma_g\}$ (see Figure 1).

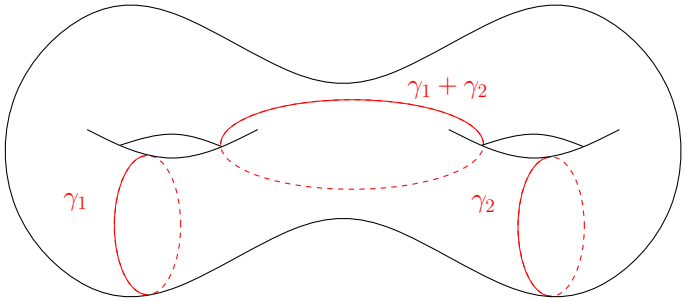

FIGURE 1. Handleslide.

This operation is called *handleslide*. Given a Heegaard decomposition $Y = U_\alpha \cup_\Sigma U_\beta$, then as above we can choose compressing discs $\boldsymbol{\alpha} = \{\alpha_1, \dots, \alpha_g\}$ and $\boldsymbol{\beta} = \{\beta_1, \dots, \beta_g\}$ on Σ for both handlebodies U_α and U_β. The data $(\Sigma, \boldsymbol{\alpha}, \boldsymbol{\beta})$ completely describes Y, and it is called a *Heegaard diagram* for Y. For example the genus 1 Heegaard decomposition of S^3 has a Heegaard diagram (T^2, α, β), where $T^2 = \{|z_1| = |z_2| = 1\}$ and the curves are $\alpha = \{|z_1| = z_2 = 1\}$ and $\beta = \{z_1 = |z_2| = 1\}$ depicted on Figure 2.

We have already seen, that isotoping and handlesliding amongst the $\boldsymbol{\alpha}$ or $\boldsymbol{\beta}$–curves does not change the described 3–manifold. Stabilizing the Heegaard decomposition can be described in terms of the Heegaard diagram as follows. Let (T^2, α, β) denote the Heegaard diagram of S^3 of Figure 2, then changing $(\Sigma, \boldsymbol{\alpha}, \boldsymbol{\beta})$ to $(\Sigma \# T^2, \boldsymbol{\alpha} \cup \{\alpha\}, \boldsymbol{\beta} \cup \{\beta\})$ corresponds to connect summing Y with S^3, thus we still get a Heegaard diagram for Y. The above described three moves are called Heegaard moves, and they form a complete set of moves:

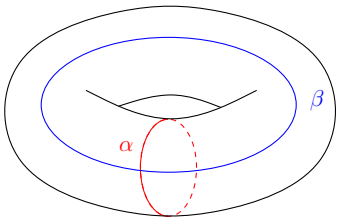

FIGURE 2. Genus 1 Heegaard diagram for S^3.

Theorem 2.1. [47, 49, 41] *Any two Heegaard diagrams* $(\Sigma_1, \boldsymbol{\alpha}_1, \boldsymbol{\beta}_1)$ *and* $(\Sigma_2, \boldsymbol{\alpha}_2, \boldsymbol{\beta}_2)$ *of* Y *have stabilizations that are related by Heegaard moves.* □

In the sequel it will be useful to fix a basepoint w in the complement of the curves in Σ. The data $(\Sigma, \boldsymbol{\alpha}, \boldsymbol{\beta}, w)$ is called a pointed Heegaard diagram. Whenever basepoints are present we require the Heegaard moves to be disjoint from them. Thus the isotopies cannot cross the basepoint, and the pair of pants of the handle slide cannot contain the basepoint and during the stabilization the connected sum is taken away from the basepoint. These restricted moves are called *pointed Heegaard moves*, and they are also sufficient:

Theorem 2.2. [47, 49, 41] *Any two pointed Heegaard diagrams* $(\Sigma_1, \boldsymbol{\alpha}_1, \boldsymbol{\beta}_1, w_1)$ *and* $(\Sigma_2, \boldsymbol{\alpha}_2, \boldsymbol{\beta}_2, w_2)$ *of* Y *have stabilizations that are related by pointed Heegaard moves.* □

The above theorems are proved using Morse theoretic arguments. Morse theory is a good way to think of Heegaard decompositions, so here follows a brief description of Morse theory and the way it defines Heegaard diagrams (for more details see [34]). Also this viewpoint allows us to generalize Heegaard Floer theories as it will be described in Subsections 2.3 and 2.5. A *Morse function* is a smooth map $f\colon Y \to \mathbb{R}$ with isolated non-degenerate critical points. In a non-degenerate critical point the Hessian is a bilinear form with no nullity. The dimension of the maximal subspace where the Hessian is negative definite is called the *index* of the critical point. The gradient flow line of the Morse function has singularities exactly in the critical points, and the index of a critical point is the dimension of its *descending manifold*; the set of points flowing up to the critical point. Thus an index λ critical point corresponds to the gluing of a 3–dimensional λ–handle. A Morse function is self-indexing if the index λ critical points lie on level λ. In the case of a closed 3–manifold a self-indexing Morse function is a function $f\colon Y \to [0,3]$

such that $f(\text{index } \lambda \text{ critical points}) = \{\lambda\}$ $(0 \leq \lambda \leq 3)$. Any smooth manifold admits a Morse function. Moreover closed manifolds admit Morse functions with only one minimum and maximum. Hereafter we will assume that $f\colon Y \to [0,3]$ is a self indexing Morse function with a unique maximum and a unique minimum. The level set $f^{-1}(\frac{3}{2}) = \Sigma$ is a genus g surface where $g = \#\{\text{index 1 critical points}\} = \#\{\text{index 2 critical points}\}$. The surface Σ is the Heegaard surface for the decomposition to two handlebodies $U_\alpha = f^{-1}[0, \frac{3}{2}]$ and $U_\beta = f^{-1}[\frac{3}{2}, 3]$. A Heegaard diagram corresponding to this Heegaard decomposition can be given as follows. The ascending manifold of an index 1 critical point intersects Σ in a connected 1 dimensional submanifold. The g index 1 critical point thus define g disjoint simple closed curves: $\boldsymbol{\alpha} = \{\alpha_1, \ldots, \alpha_g\}$ Similarly the intersection of the descending manifolds of the index 2 critical points define the curves $\boldsymbol{\beta} = \{\beta_1, \ldots, \beta_g\}$ on the surface Σ. With the above notations the diagram $(\Sigma, \boldsymbol{\alpha}, \boldsymbol{\beta})$ is a Heegaard diagram for Y. A basepoint w on Σ gives a gradient flowline connecting the minimum to the maximum.

Theorem 2.2 gives us a way to define 3–manifold invariants using Heegaard diagrams. An invariant of (pointed) Heegaard diagrams that is invariant under (pointed) Heegaard moves, is a 3–manifold invariant. This is the idea Ozsváth and Szabó followed to define Heegaard Floer homologies.

2.2. **Symmetric product, holomorphic discs.** In the sequel it will be useful to understand certain structures associated to a pointed Heegaard diagram $(\Sigma, \boldsymbol{\alpha}, \boldsymbol{\beta}, w)$. The gth *symmetric product* of Σ is: $\mathrm{Sym}^g(\Sigma) = \Sigma^{\times g}/S_g$, where S_g is the symmetric group on g letters acting by permuting the coordinates. Although S_g does not act freely on the product, the symmetric product turns out to be a smooth $2g$ dimensional manifold, moreover it inherits a complex structure from a complex structure on Σ. The $\boldsymbol{\alpha}$ and $\boldsymbol{\beta}$–curves define totally real tori $\mathbb{T}_\alpha = \alpha_1 \times \cdots \times \alpha_g$ and $\mathbb{T}_\beta = \beta_1 \times \cdots \times \beta_g \subseteq \mathrm{Sym}^g(\Sigma)$ and the basepoint defines the divisor $V_w = \{w\} \times \mathrm{Sym}^{g-1}(\Sigma)$ disjoint from the tori. If the $\boldsymbol{\alpha}$ and $\boldsymbol{\beta}$–curves are transversal in Σ, then the tori $\mathbb{T}_\alpha$ and $\mathbb{T}_\beta$ intersect each other transversally too. Thus the intersection is a compact 0 dimensional manifold. The Heegaard Floer chain complex will be generated by these intersection points $\mathbb{T}_\alpha \cap \mathbb{T}_\beta$. In other words the generators are g-tuples of points of Σ, such that there is exactly one point on each α and β curve.

The boundary map is defined using holomorphic discs. Consider the disc $\mathbb{D} = \{|z| \leq 1\} \subseteq \mathbb{C}$. Divide its boundary to two arcs $e_\alpha = \partial\mathbb{D} \cap \{\mathrm{Re}(z) \geq 0\}$ and $e_\beta = \partial\mathbb{D} \cap$

$\{\mathrm{Re}(z) \leq 0\}$. For two intersection points $\mathbf{x}, \mathbf{y} \in \mathrm{Sym}^g(\Sigma)$ the set $\pi_2(\mathbf{x}, \mathbf{y})$ consists of homotopy classes of maps $\phi\colon \mathbb{D} \to \mathrm{Sym}^g(\Sigma)$ such that $\phi(-i) = \mathbf{x}$, $\phi(i) = \mathbf{y}$, $\phi(e_\alpha) \subseteq \mathbb{T}_\alpha$ and $\phi(e_\beta) \subseteq \mathbb{T}_\beta$. (See Figure 3 for a schematic picture.) Note that there is no

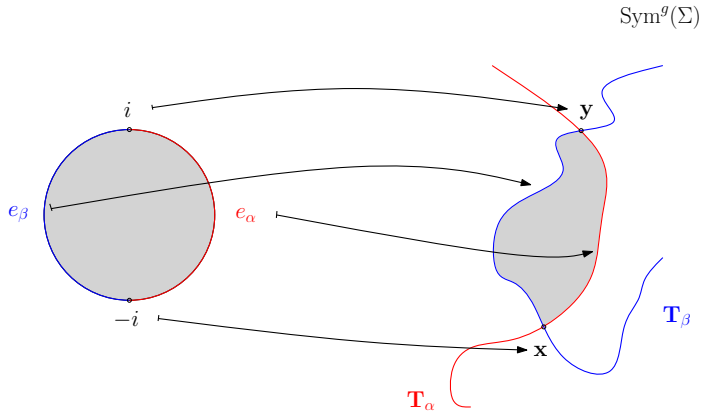

FIGURE 3. A Whitney disc.

multiplication on $\pi_2(\mathbf{x}, \mathbf{y})$ unless $\mathbf{x} = \mathbf{y}$. To understand the boundary maps better we consider their "shadow" on Σ. For any point z on Σ define the divisor $V_z = \{z\} \times \mathrm{Sym}^{g-1}(\Sigma)$ and for a map $\phi \in \pi_2(\mathbf{x}, \mathbf{y})$ let $n_z(\phi) = \#\{V_z \cap \phi(\mathbb{D})\}$. Choose a point z_i in each component $\mathcal{D}_i$ of $\Sigma - \cup\boldsymbol{\alpha} - \cup\boldsymbol{\beta}$ then the domain of a map $\phi \in \pi_2(\mathbf{x}, \mathbf{y})$ is $\mathcal{D}(\phi) = \sum n_{z_i}(\phi)\mathcal{D}_i$. This is independent of the choice of the z_i's and the chosen representation of the homotopy class. Its boundary $\partial\mathcal{D}$ consist of subarcs of the $\boldsymbol{\alpha}$- and $\boldsymbol{\beta}$–curves connecting the tuples $\mathbf{x}$ to $\mathbf{y}$ on the $\boldsymbol{\alpha}$–curves and $\mathbf{y}$ to $\mathbf{x}$ on the $\boldsymbol{\beta}$–curves. A domain satisfying the latter conditions is said to connect $\mathbf{x}$ to $\mathbf{y}$. Note that if the homotopy class ϕ contains a holomorphic representative, then $n_z(\phi) \geq 0$ for any $z \in \Sigma$. The difference of two domains connecting $\mathbf{x}$ to $\mathbf{y}$ is a domain whose boundary contain full $\boldsymbol{\alpha}$ and $\boldsymbol{\beta}$–curves. Such domains are called *periodic domains*. A Heegaard diagram is *weakly admissible* if all nontrivial periodic domains have components with both positive and negative coefficient. Weak admissibility ensures the finiteness of homotopy classes with holomorphic representatives connecting $\mathbf{x}$ to $\mathbf{y}$. Every Heegaard diagram is isotopic to a weakly admissible one. In the sequel without explicitly stating we will always assume that Heegaard diagrams at issue are weakly admissible. For a fixed homotopy class $\phi \in \pi_2(\mathbf{x}, \mathbf{y})$ consider the moduli space of holomorphic discs $\mathcal{M}(\phi)$ representing ϕ. Note that in order to guarantee the smoothness of $\mathcal{M}(\phi)$ one needs to

perturb the inherited complex structure on $\mathrm{Sym}^g(\Sigma)$. This is where Lagrangian Floer homology comes into the picture, and in this dissertation we will only use the results coming from this theory, without introducing any of the tools (See [17, 18] for details). The dimension of $\mathcal{M}(\phi)$ is called the Maslov index of ϕ, and is denoted by $\mu(\phi)$. Note that $\mathbb{D}$ is conform equivalent to the strip $[-1,1]\times\mathbb{R}$ with e_α and e_β being mapped to $\{1\}\times\mathbb{R}$ and $\{-1\}\times\mathbb{R}$, thus translations provide an $\mathbb{R}$-action on the moduli space $\mathcal{M}(\phi)$.

2.3. **Heegaard Floer homology.** Suppose that Y is a smooth oriented 3–manifold, and $(\Sigma,\boldsymbol{\alpha},\boldsymbol{\beta},w)$ is a Heegaard diagram for Y. Consider the module $\mathrm{CF}^-(\Sigma,\boldsymbol{\alpha},\boldsymbol{\beta},w)$ over the polynomial algebra $\mathbb{Z}_2[U]$ freely generated by the intersection points of the totally real submanifolds $\mathbb{T}_\alpha=\alpha_1\times\cdots\times\alpha_g$ and $\mathbb{T}_\beta=\beta_1\times\cdots\times\beta_g$ of $\mathrm{Sym}^g(\Sigma)$. This module is endowed with the differential

$$\partial^-\mathbf{x}=\sum_{\mathbf{y}\in\mathbb{T}_\alpha\cap\mathbb{T}_\beta}\sum_{\substack{\phi\in\pi_2(\mathbf{x},\mathbf{y})\\ \mu(\phi)=1}}\left|\frac{\mathcal{M}(\phi)}{\mathbb{R}}\right|U^{n_w(\phi)}\mathbf{y}$$

The relative Maslov-grading of two intersection points $\mathbf{x},\mathbf{y}\in\mathbb{T}_\alpha\cap\mathbb{T}_\beta$ is defined by $M(\mathbf{x})-M(\mathbf{y})=\mu(\phi)-2n_w(\phi)$, where $\phi\in\pi_2(\mathbf{x},\mathbf{y})$ is any homotopy class from $\mathbf{x}$ to $\mathbf{y}$. We extend this relative grading to the whole module by $M(U^a\mathbf{x})=M(\mathbf{x})-2a$. The differential ∂^- lowers the grading by 1. By examining the boundary of 1 dimensional moduli spaces of holomorphic discs it is proved:

Theorem 2.3 (Ozsváth-Szabó, [41])**.** $(\mathrm{CF}^-,\partial^-)$ *is a chain-complex, i.e.* $(\partial^-)^2=0$. □

Thus we can take its homology $\mathrm{HF}^-(\Sigma,\boldsymbol{\alpha},\boldsymbol{\beta},w)$. As it was shown in [41], the homotopy type of the chain complex is invariant under pointed Heegaard moves, and thus give an invariant for Y.

Theorem 2.4 (Ozsváth-Szabó, [41])**.** *Let Y be a closed oriented 3–manifold. Consider the Heegaard diagrams $(\Sigma_1,\boldsymbol{\alpha}_1,\boldsymbol{\beta}_1,w_1)$ and $(\Sigma_2,\boldsymbol{\alpha}_2,\boldsymbol{\beta}_2,w_2)$ for Y. Then the complexes $\mathrm{CF}^-(\Sigma_1,\boldsymbol{\alpha}_1,\boldsymbol{\beta}_1,w_1)$ and $\mathrm{CF}^-(\Sigma_2,\boldsymbol{\alpha}_2,\boldsymbol{\beta}_2,w_2)$ are chain-homotopy equivalent as $\mathbb{Z}_2[U]$-modules. In particular $\mathrm{HF}^-(\Sigma_1,\boldsymbol{\alpha}_1,\boldsymbol{\beta}_1,w_1)$ and $\mathrm{HF}^-(\Sigma_2,\boldsymbol{\alpha}_2,\boldsymbol{\beta}_2,w_2)$ are isomorphic.*

A simpler version of the above invariant is gotten by setting $U=0$. In other words, the chain complex $\widehat{CF}$ is generated by $\mathbb{T}_\alpha\cap\mathbb{T}_\beta$ over $\mathbb{Z}_2$, and the boundary map is given

by:

$$\hat{\partial}\mathbf{x} = \sum_{\mathbf{y}\in\mathbb{T}_\alpha\cap\mathbb{T}_\beta} \sum_{\substack{\phi\in\pi_2(\mathbf{x},\mathbf{y})\\ \mu(\phi)=1\\ n_z(\phi)=0}} \left|\frac{\mathcal{M}(\phi)}{\mathbb{R}}\right| \mathbf{y}$$

This defines a chain-complex, and as a consequence of Theorem 2.4, its chain homotopy type and thus its homology only depends on the 3–manifold Y:

Theorem 2.5 (Ozsváth-Szabó, [41])**.** *Let Y be a closed oriented 3–manifold. Consider the Heegaard diagrams $(\Sigma_1, \boldsymbol{\alpha}_1, \boldsymbol{\beta}_1, w_1)$ and $(\Sigma_2, \boldsymbol{\alpha}_2, \boldsymbol{\beta}_2, w_2)$ for Y. Then the complexes $\widehat{CF}(\Sigma_1, \boldsymbol{\alpha}_1, \boldsymbol{\beta}_1, w_1)$ and $\widehat{CF}(\Sigma_2, \boldsymbol{\alpha}_2, \boldsymbol{\beta}_2, w_2)$ are chain-homotopy equivalent as $\mathbb{Z}_2$-vectorspaces. In particular $\widehat{HF}(\Sigma_1, \boldsymbol{\alpha}_1, \boldsymbol{\beta}_1, w_1)$ and $\widehat{HF}(\Sigma_2, \boldsymbol{\alpha}_2, \boldsymbol{\beta}_2, w_2)$ are isomorphic.*

2.4. **Knot Floer homology.** Here we outline the basic definitions of knot Floer homologies, originally defined by Ozsváth and Szabó [44] and independently by Rasmussen [46]. Let K be an oriented null homologous knot in a 3–manifold Y. Fix a Morse function $K \to [0,3]$ with a unique minimum at level 0 and a unique maximum at level 3. This function can be extended to a self-indexing Morse function for the entire manifold with no additional minima and maxima. Then K intersects the Heegaard surface Σ in exactly two points. The positive intersection point is called z, the negative one is w. Thus we get a Heegaard diagram $(\Sigma, \boldsymbol{\alpha}, \boldsymbol{\beta}, w, z)$ with two basepoints. Conversely, if a Heegaard diagram with two basepoints is given, then we can recover the 3–manifold and the knot in it as follows. By connecting the basepoints w and z in the complement of the $\boldsymbol{\alpha}$–curves and z to w in the complement of the $\boldsymbol{\beta}$–curves we get two arcs on Σ, the former one can be pushed into U_α and the latter one to U_β, to form an embedded knot K in Y. (See Figure 4 for a Heegaard diagram associated to the right handed trefoil knot in S^3.) Thanks to the new basepoint, the same chain complex $(\mathrm{CF}^-, \partial^-)$ now admits an additional relative grading A called the *Alexander grading*. For two intersection points $\mathbf{x}, \mathbf{y} \in \mathrm{Sym}^g(\Sigma)$ the Alexander grading difference is $A(\mathbf{x}) - A(\mathbf{y}) = n_z(\phi) - n_w(\phi)$, where $\phi \in \pi_2(\mathbf{x}, \mathbf{y})$. This is independent of ϕ provided that K was null homologous. The homology of the graded complex $(CFK^- = \mathrm{CF}^-, \partial_0^-)$ with

$$\partial_0^-\mathbf{x} = \sum_{\mathbf{y}\in\mathbb{T}_\alpha\cap\mathbb{T}_\beta} \sum_{\substack{\phi\in\pi_2(\mathbf{x},\mathbf{y})\\ \mu(\phi)=1\\ n_z(\phi)=0}} \left|\frac{\mathcal{M}(\phi)}{\mathbb{R}}\right| U^{n_w(\phi)}\mathbf{y}$$

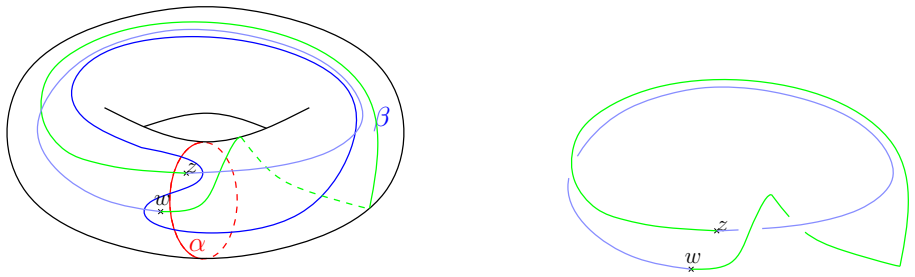

Heegaard diagram The knot

FIGURE 4. Heegaard diagram of the right handed trefoil knot.

is an invariant of the pair (Y, K). As before, a simpler version $\widehat{\mathrm{HFK}}$ can also be defined by setting $U = 0$ in the previous equation.

Theorem 2.6 (Ozsváth-Szabó, [39])**.** *Let K be a null homologous knot in a closed oriented 3–manifold Y. Consider the Heegaard diagrams $(\Sigma_1, \boldsymbol{\alpha}_1, \boldsymbol{\beta}_1, w_1, z_1)$ and $(\Sigma_2, \boldsymbol{\alpha}_2, \boldsymbol{\beta}_2, w_2, z_2)$ for the pair (Y, K). Then the complexes $CFK^-(\Sigma_1, \boldsymbol{\alpha}_1, \boldsymbol{\beta}_1, w_1, z_1)$ and $CFK^-(\Sigma_2, \boldsymbol{\alpha}_2, \boldsymbol{\beta}_2, w_2, z_2)$ are chain-homotopy equivalent as $\mathbb{Z}_2[U]$-modules. In particular $\mathrm{HFK}^-(\Sigma_1, \boldsymbol{\alpha}_1, \boldsymbol{\beta}_1, w_1, z_1)$ and $\mathrm{HFK}^-(\Sigma_2, \boldsymbol{\alpha}_2, \boldsymbol{\beta}_2, w_2, z_2)$ are isomorphic. Similar statement holds for the $\widehat{\mathrm{HFK}}$ theories.*

2.5. **Heegaard Floer homologies with multiple basepoints.** A more general description of knot Floer homology, using multiple basepoints is used to define the combinatorial version of knot Floer homology in S^3. (See Subsection **??**.) Here we briefly outline the definition, and then restrict ourselves to knots only in S^3, as this will be the context we will need later. Consider a knot K in an oriented, closed 3–manifold Y. There is a self-indexing Morse function with k minima and k maxima such that K is made out of $2k$ flow lines connecting all the index zero and index three critical points. Such a Morse function gives rise to a Heegaard diagram $(\Sigma, \boldsymbol{\alpha}, \boldsymbol{\beta}, \mathbf{w}, \mathbf{z})$ for (Y, K) in the following way. Let $\Sigma = f^{-1}(\frac{3}{2})$ be a genus g surface. The $\boldsymbol{\alpha}$–curves $\boldsymbol{\alpha} = \{\alpha_1, \dots, \alpha_{g+k-1}\}$ are defined to be the circles of Σ whose points flow down to the index one critical points. Similarly $\boldsymbol{\beta} = \{\beta_1, \dots, \beta_{g+k-1}\}$ are the curves with points flowing up to the index two critical points. Finally let $\mathbf{z} = \{z_1, \dots, z_k\}$ be the positive intersection points and $\mathbf{w} = \{w_1, \dots, w_k\}$ be the negative intersection points of K with Σ.

Consider the module $\mathrm{CF}^-(\Sigma, \boldsymbol{\alpha}, \boldsymbol{\beta}, \mathbf{w})$ over the polynomial algebra $\mathbb{Z}_2[U_1, \dots, U_k]$ freely generated by the intersection points of the totally real submanifolds $\mathbb{T}_\alpha = \alpha_1 \times \cdots \times \alpha_{g+k-1}$ and $\mathbb{T}_\beta = \beta_1 \times \cdots \times \beta_{g+k-1}$ of $\mathrm{Sym}^{g+k-1}(\Sigma)$. This module is endowed with the differential

$$\partial^- \mathbf{x} = \sum_{\mathbf{y} \in \mathbb{T}_\alpha \cap \mathbb{T}_\beta} \sum_{\substack{\phi \in \pi_2(\mathbf{x}, \mathbf{y}) \\ \mu(\phi) = 1}} \left| \frac{\mathcal{M}(\phi)}{\mathbb{R}} \right| U_1^{n_{w_1}(\phi)} \cdots U_k^{n_{w_k}(\phi)} \mathbf{y}$$

Let

$$\left(\widehat{\mathrm{CF}}(\Sigma, \boldsymbol{\alpha}, \boldsymbol{\beta}, \mathbf{w}), \widehat{\partial} \right) = \left(\frac{\mathrm{CF}^-(\Sigma, \boldsymbol{\alpha}, \boldsymbol{\beta}, \mathbf{w})}{(U_1 = 0)}, \left[\partial^- \right] \right). \tag{1}$$

The chain-homotopy type of the above complexes are invariants of Y in the following sense:

Theorem 2.7. *(Ozsváth-Szabó, [44]) Let Y be a closed oriented 3–manifold. Consider the Heegaard diagrams $(\Sigma_1, \boldsymbol{\alpha}_1, \boldsymbol{\beta}_1, \mathbf{w}_1)$ and $(\Sigma_2, \boldsymbol{\alpha}_2, \boldsymbol{\beta}_2, \mathbf{w}_2)$ for Y with $|\mathbf{w}_1| = k_1$ and $|\mathbf{w}_2| = k_2$. Assuming $k_1 \geq k_2$ the complexes $\mathrm{CF}^-(\Sigma_1, \boldsymbol{\alpha}_1, \boldsymbol{\beta}_1, \mathbf{w}_1)$ and $\mathrm{CF}^-(\Sigma_2, \boldsymbol{\alpha}_2, \boldsymbol{\beta}_2, \mathbf{w}_2)$ are chain-homotopy equivalent as $\mathbb{Z}_2[U_1, \dots, U_{k_1}]$-modules. Here the latter complex is endowed with the $\mathbb{Z}_2[U_1, \dots, U_{k_1}]$-module structure by defining the action of $U_{k_2}, \dots, U_{k_1}$ to be identical. Similar statement holds for the $\widehat{\mathrm{CF}}$-theory, moreover the chain-homotopy equivalences form a commutative diagram with the factorization map of (1).* □

Hereafter we assume that our underlying 3–manifold is the 3–sphere. Note that in this case the homology of $\mathrm{CF}^-(\Sigma, \boldsymbol{\alpha}, \boldsymbol{\beta}, \mathbf{w})$ is $\mathrm{HF}^-(S^3) = \mathbb{Z}_2[U]$. The relative Maslov-grading of two intersection points $\mathbf{x}, \mathbf{y} \in \mathbb{T}_\alpha \cap \mathbb{T}_\beta$ is defined by $M(\mathbf{x}) - M(\mathbf{y}) = \mu(\phi) - 2 \sum n_{w_i}(\phi)$, where $\phi \in \pi_2(\mathbf{x}, \mathbf{y})$ is any homotopy class from $\mathbf{x}$ to $\mathbf{y}$. Since knots in S^3 are nullhomologous this grading is independent of the chosen homotopy class. We extend this relative grading to the whole module by $M(U_1^{a_1} \cdots U_k^{a_k} \mathbf{x}) = M(\mathbf{x}) - 2(a_1 + \cdots + a_k)$. For S^3, the grading can be lifted to an absolute grading by fixing the grading of the generator of $\mathrm{HF}^-(S^3) = \mathbb{Z}_2[U]$ at 0.

Note that so far we made no reference to the basepoints $\mathbf{z}$. The relative Alexander grading is defined by $A(\mathbf{x}) - A(\mathbf{y}) = \sum n_{z_i}(\phi) - \sum n_{w_i}(\phi)$, where again ϕ can be chosen to be any homotopy class in $\pi_2(\mathbf{x}, \mathbf{y})$. This relative grading can be uniquely lifted to an absolute Alexander grading which satisfies $\sum T^{A(x)} = \Delta_K(T)(1-T)^{n-1} \pmod 2$,

where $\Delta_K(T)$ is the symmetrized Alexander polynomial. We can extend the Alexander grading to the module by $A(U_1^{a_1}\cdots U_k^{a_k}\mathbf{x}) = A(\mathbf{x}) - (a_1+\cdots+a_k)$. As the local multiplicities of pseudo-holomorphic discs are non-negative, we obtain filtered chain complexes $CFK^-(\Sigma,\boldsymbol{\alpha},\boldsymbol{\beta},\mathbf{w},\mathbf{z})$ and $\widehat{\mathrm{CFK}}(\Sigma,\boldsymbol{\alpha},\boldsymbol{\beta},\mathbf{w},\mathbf{z})$, that are invariants of the knot:

Theorem 2.8. *(Ozsváth–Szabó, [44]) Let K be an oriented knot. Consider the Heegaard diagrams $(\Sigma_1,\boldsymbol{\alpha}_1,\boldsymbol{\beta}_1,\mathbf{w}_1,\mathbf{z}_1)$ and $(\Sigma_2,\boldsymbol{\alpha}_2,\boldsymbol{\beta}_2,\mathbf{w}_2,\mathbf{z}_2)$ for K with $|\mathbf{w}_1| = |\mathbf{z}_1| = k_1$ and $|\mathbf{w}_2| = |\mathbf{z}_2| = k_2$. Assuming $k_1 \geq k_2$ the filtered complexes $CFK^-(\Sigma_1,\boldsymbol{\alpha}_1,\boldsymbol{\beta}_1,\mathbf{w}_1,\mathbf{z}_1)$ and $CFK^-(\Sigma_2,\boldsymbol{\alpha}_2,\boldsymbol{\beta}_2,\mathbf{w}_2,\mathbf{z}_2)$ are filtered chain-homotopy equivalent as $\mathbb{Z}_2[U_1,\dots,U_{k_1}]$-modules. Here the latter complex is endowed with the $\mathbb{Z}_2[U_1,\dots,U_{k_1}]$-module structure by defining the action of $U_{k_2},\dots,U_{k_1}$ to be identical. Similar statement holds for the $\widehat{\mathrm{CFK}}$-theory, moreover the chain homotopy equivalences form a commutative diagram with the factorization map of (1).* □

As it is easier to work with, we usually consider the associated graded objects of the filtered chain complexes and denote their homologies by HFK^-. In particular $HFK^-(\Sigma,\boldsymbol{\alpha},\boldsymbol{\beta},\mathbf{w},\mathbf{z})$ is the homology of the complex $(CFK^-(\Sigma,\boldsymbol{\alpha},\boldsymbol{\beta},\mathbf{w},\mathbf{z}),\partial_0^-)$, where

$$\partial_0^-\mathbf{x} = \sum_{\mathbf{y}\in\mathbb{T}_\alpha\cap\mathbb{T}_\beta}\ \sum_{\substack{\phi\in\pi_2(\mathbf{x},\mathbf{y})\\ n_{z_1}(\phi)+\cdots+n_{z_k}(\phi)=0\\ \mu(\phi)=1}} \left|\frac{\mathcal{M}(\phi)}{\mathbb{R}}\right| U_1^{n_{w_1}(\phi)}\cdots U_k^{n_{w_k}(\phi)}\mathbf{y}.$$

The U_i's for different i act chain-homotopically, so on the homology level all U_i act identically. This observation endows $HFK^-(\Sigma,\boldsymbol{\alpha},\boldsymbol{\beta},\mathbf{w},\mathbf{z})$ with a $\mathbb{Z}_2[U]$-structure, by defining the U action to be the action of any of the U_i's. Then Theorem 2.8 translates:

Theorem 2.9. *(Ozsváth–Szabó, [44]) Let K be an oriented knot. Consider the Heegaard diagrams $(\Sigma_1,\boldsymbol{\alpha}_1,\boldsymbol{\beta}_1,\mathbf{w}_1,\mathbf{z}_1)$ and $(\Sigma_2,\boldsymbol{\alpha}_2,\boldsymbol{\beta}_2,\mathbf{w}_2,\mathbf{z}_2)$ for K. Then the knot Floer homologies $\mathrm{HFK}^-(\Sigma_1,\boldsymbol{\alpha}_1,\boldsymbol{\beta}_1,\mathbf{w}_1,\mathbf{z}_1)$ and $\mathrm{HFK}^-(\Sigma_2,\boldsymbol{\alpha}_2,\boldsymbol{\beta}_2,\mathbf{w}_2,\mathbf{z}_2)$ are isomorphic as $\mathbb{Z}_2[U]$-modules. Similar statement holds for the $\widehat{\mathrm{HFK}}$-theory, moreover the isomorphisms form a commutative diagram with the factorization map of (1).* □

Knot Floer homology satisfies a Künneth-type formula for connected sums:

Theorem 2.10. *(Ozsváth–Szabó, [44]) Let K_1 and K_2 be oriented knots in S^3 described by the Heegaard diagrams $(\Sigma_1,\boldsymbol{\alpha}_1,\boldsymbol{\beta}_1,\mathbf{w}_1,\mathbf{z}_1)$ and $(\Sigma_2,\boldsymbol{\alpha}_2,\boldsymbol{\beta}_2,\mathbf{w}_2,\mathbf{z}_2)$. Let $w\in\mathbf{w}_1$ and $z\in\mathbf{z}_2$. Then*

(1) $(\Sigma_1\#\Sigma_2, \boldsymbol{\alpha}_1 \cup \boldsymbol{\alpha}_2, \boldsymbol{\beta}_1 \cup \boldsymbol{\beta}_2, (\mathbf{w}_1 - w) \cup \mathbf{w}_2, \mathbf{z}_1 \cup (\mathbf{z}_2 - z))$ *is a Heegaard diagram for* $K_1\#K_2$. *Here the connected sum* $\Sigma_1\#\Sigma_2$ *is taken in the regions containing* $w \in \Sigma_1$ *and* $z \in \Sigma_2$;

Let $|\mathbf{w}_1| = |\mathbf{z}_1| = k_1$ *and* $|\mathbf{w}_2| = |\mathbf{z}_2| = k_2$. *Both complexes* $CFK^-(\Sigma_1, \boldsymbol{\alpha}_1, \boldsymbol{\beta}_1, \mathbf{w}_1, \mathbf{z}_1)$ *and* $CFK^-(\Sigma_2, \boldsymbol{\alpha}_2, \boldsymbol{\beta}_2, \mathbf{w}_2, \mathbf{z}_2)$ *are* $\mathbb{Z}_2[U_1, \dots, U_{k_1}, V_1, \dots, V_{k_2}]$*-modules with the elements* $U_1, \dots, U_{k_1}$ *acting trivially on the latter and* $V_1, \dots, V_{k_2}$ *acting trivially on the former complex. With these conventions in place we have*

(2) $CFK^-(\Sigma_1, \boldsymbol{\alpha}_1, \boldsymbol{\beta}_1, \mathbf{w}_1, \mathbf{z}_1) \otimes_{U_1=V_1} CFK^-(\Sigma_2, \boldsymbol{\alpha}_2, \boldsymbol{\beta}_2, \mathbf{w}_2, \mathbf{z}_2)$ *is filtered chain homotopy equivalent to*

$$CFK^-(\Sigma_1\#\Sigma_2, \boldsymbol{\alpha}_1 \cup \boldsymbol{\alpha}_2, \boldsymbol{\beta}_1 \cup \boldsymbol{\beta}_2, (\mathbf{w}_1 - w) \cup \mathbf{w}_2, \mathbf{z}_1 \cup (\mathbf{z}_2 - z));$$

(3) $\mathrm{HFK}^-(K_1\#K_2)$ *is isomorphic to* $\mathrm{HFK}^-(K_1) \otimes \mathrm{HFK}^-(K_2)$ *and this isomorphism can be given by* $\mathbf{x}_1 \otimes \mathbf{x}_2 \mapsto (\mathbf{x}_1, \mathbf{x}_2)$ *on the generators.*

Similar statement holds for the $\widehat{\mathrm{CFK}}$*-theory, moreover the chain homotopy equivalences form a commutative diagram with the factorization map of (1).* □

2.6. **Combinatorial knot Floer homology and grid diagrams.** As it was observed in [32, 31], knot Floer homology admits a completely combinatorial description via grid diagrams. A *grid diagram* G is a $k \times k$ square grid placed on the plane with some of its cells decorated with an X or an O and containing exactly one X and O in each of its rows and columns. Such a diagram naturally defines an oriented link projection by connecting the O's to the X's in each row and the X's to the O's in the columns and letting the vertical line to overpass at the intersection points. For simplicity we will assume that the corresponding link is a knot K. There are certain moves of the grid diagram that do not change the (topological) knot type [45]. These are *cyclic permutation* of the rows or columns, *commutation* of two consecutive rows (columns) such that the X and the O from one row (column) does not separate the X and the O from the other row (column) and *(de)stabilization* which is defined as follows. A square in the grid containing an X (O) can be subdivided into four squares by introducing a new vertical and a new horizontal line dividing the row and the column that contains that square. By replacing the X (O) by one O (X) and two X's (O's) in the diagonal of the new four squares and placing the two O's (X's) in the subdivided row and column appropriately, we get a new grid diagram which is called the stabilization of

the original one. The inverse of stabilization is destabilization. There are eight types of (de)stabilization: $O:SW$, $O:SE$, $O:NW$, $O:NE$, $X:SW$, $X:SE$, $X:NW$ and $X:NE$, where the first coordinate indicates which symbol we started with and the second shows the placement of the unique new symbol. A stabilization of type $X:NW$ is depicted on Figure 5.

Placing the grid on a torus by identifying the opposite edges of the square grid we obtain a Heegaard diagram with multiple basepoints for (S^3, K). Here the $\mathbf{w}$'s correspond to the O's, the $\mathbf{z}$'s to the X's, and the $\boldsymbol{\alpha}$–curves to the horizontal lines and the $\boldsymbol{\beta}$–curves to the vertical lines. As each region of this Heegaard diagram is a square, it is"nice" in the sense defined in [48]. Thus boundary maps can be given by rectangles. This observation led to a completely combinatorial description of knot Floer homology [32, 31] in the 3–sphere.

2.7. **Sutured Floer homology.** A *sutured 3–manifold* is a pair (Y, γ) where Y is a compact, oriented 3–manifold with boundary and $\gamma \subset \partial Y$ is a disjoint set of embedded tori and annuli. Every component of $R(\gamma) = \partial Y - \gamma$ is oriented, and R_+ (resp. R_-) is the union of those components where the normal vector points out (resp. in) Y. The sutured manifold is called *balanced* if all sutures are annular, Y has no closed components, every boundary component admits a suture and $\chi(R_+) = \chi(R_-)$ on every component of Y. As is customary, annular sutures are symbolized by the homologically nontrivial simple closed curves they contain, the collection of which is denoted by Γ. Without confusion, the term "suture" will also refer to these homologically nontrivial curves, and sometimes to their union Γ. The suture Γ is oriented as the boundary of $R_+ \subset \partial Y$. We will consider only balanced sutured manifolds.

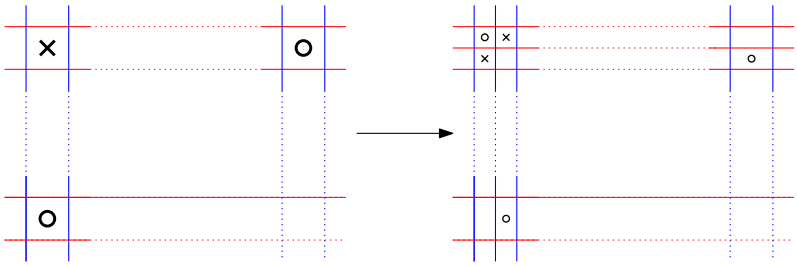

FIGURE 5. Stabilization of type $X:NW$

Heegaard diagrams can be generalized to this context as follows. Any balanced sutured 3-manifold admits a self-indexing Morse-function $f : Y \to [-1, 4]$ with $f^{-1}(-1) = R_-$, $f^{-1}(4) = R_+$, $f^{-1}(\frac{3}{2}) \cap \partial Y = \Gamma$ and f being the height function for a trivialization of $\gamma = \nu(\Gamma) = \Gamma \times I \to I$. A Morse-function on Y gives rise to a *balanced Heegaard diagram*, $(\Sigma, \boldsymbol{\alpha}, \boldsymbol{\beta})$ for Y in the usual manner. $\Sigma = f^{-1}(\frac{3}{2})$ is a surface with no closed components and with boundary Γ. Then the $\boldsymbol{\alpha}$–curves are the ones that are flowing down to the index 1 critical points at infinity, while the $\boldsymbol{\beta}$–curves are the ones to which the index 2 critical points are flowing up to with the flow of a gradient-like vector field. Note that both the $\boldsymbol{\alpha}$–curves and the $\boldsymbol{\beta}$–curves are homologically independent and disjoint. Also as (Y, Γ) is balanced, we have $|\boldsymbol{\alpha}| = |\boldsymbol{\beta}| =: k$. As it is proved by Juhász, a balanced Heegaard diagram corresponds to a balanced sutured 3–manifold if and only if $|\boldsymbol{\alpha}| = |\boldsymbol{\beta}|$ and the maps $\pi_0(\partial\Sigma) \to \pi_0(\Sigma - \boldsymbol{\alpha})$ and $\pi_0(\partial\Sigma) \to \pi_0(\Sigma - \boldsymbol{\beta})$ are surjective. For a given set of curves $\boldsymbol{\gamma} = \{\gamma_1, \dots, \gamma_k\}$ on Σ denote by $\Sigma[\boldsymbol{\gamma}]$ the surface obtained by surgery on Σ along $\boldsymbol{\gamma}$.

The previous scheme applies verbatim (without even the choice of base points). Consider the module $\mathrm{SFC}(\Sigma, \boldsymbol{\alpha}, \boldsymbol{\beta})$ freely generated over $\mathbb{Z}_2$ by the intersection points of the totally real submanifolds $\mathbb{T}_\alpha = \alpha_1 \times \cdots \times \alpha_k$ and $\mathbb{T}_\beta = \beta_1 \times \cdots \times \beta_k$ of $\mathrm{Sym}^k(\Sigma)$. This module is endowed with the differential:

$$\partial \mathbf{x} = \sum_{\mathbf{y} \in \mathbb{T}_\alpha \cap \mathbb{T}_\beta} \sum_{\substack{\phi \in \pi_2(\mathbf{x}, \mathbf{y}) \\ \phi \cap \Gamma \times \mathrm{Sym}^k(\Sigma) = \emptyset \\ \mu(\phi) = 1}} \left| \frac{\mathcal{M}(\phi)}{\mathbb{R}} \right| \mathbf{y}$$

Weak admissibility ensures the above sum to be finite. Denote the homology of the complex by $\mathrm{SFH}(\Sigma, \boldsymbol{\alpha}, \boldsymbol{\beta})$.

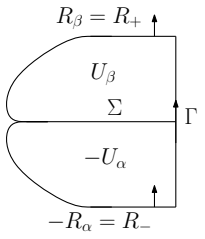

FIGURE 6. Schematic picture for a balanced sutured 3-manifold

Theorem 2.11 (Juhász, [26]). *Suppose that* $(\Sigma_1, \boldsymbol{\alpha}_1, \boldsymbol{\beta}_1)$ *and* $(\Sigma_2, \boldsymbol{\alpha}_2, \boldsymbol{\beta}_2)$ *are balanced Heegaard diagrams for the same balanced sutured 3-manifold* (Y, Γ)*. Then there is an induced* $\mathbb{Z}_2$*-module isomorphism for the corresponding sutured Floer homologies:*

$$\Psi : \mathrm{SFH}(\Sigma_1, \boldsymbol{\alpha}_1, \boldsymbol{\beta}_1), \to \mathrm{SFH}(\Sigma_2, \boldsymbol{\alpha}_2, \boldsymbol{\beta}_2).$$

□

The above defined invariant is the *sutured Floer homology* $\mathrm{SFH}(Y, \Gamma)$. This theory is a common generalization of the $\widehat{\mathrm{HF}}$ and $\widehat{\mathrm{HFK}}$ theories. Indeed, if $(\Sigma, \boldsymbol{\alpha}, \boldsymbol{\beta}, w)$ is a pointed Heegaard diagram for a 3–manifold, then by deleting a small neighborhood $\nu(w)$ of w from Σ, we obtain a balanced sutured Heegaard diagram $(\Sigma - \nu(w), \boldsymbol{\alpha}, \boldsymbol{\beta})$ for $Y - B^3$ with a one component suture Γ on its boundary S^2. The definitions of the corresponding Heegaard theories are literally the same, thus $\widehat{\mathrm{HF}}(Y)$ is isomorphic to $\mathrm{SFH}(Y - B^3, \Gamma)$. The same principle generalizes for knots too, which we will describe from another perspective. If Σ has exactly two boundary components and $\overline{\Sigma}$ denotes the capped of closed surface, and if the number of attaching curves k equals to the genus of Σ and the curves are homologically independent in $\overline{\Sigma}$, then the corresponding sutured 3–manifold has toric boundary with a 2–component suture, and by placing two marked points on the caps we get an identification

$$\Phi \colon \mathrm{SFH}(Y, \Gamma) \to \widehat{\mathrm{HFK}}(Y_\Gamma, K'),$$

where Y_Γ is the result of Dehn filling of Y with slope given by a component of Γ and K' is the core of the glued–up solid torus.

3. Contact 3–manifolds

Here we give a brief overview of the necessary definitions and notions of contact topology. For a more complete treatment the reader is referred to [13, 36]. A *contact structure* ξ on an oriented 3–manifold Y is a totally non-integrable plane field. In other words it is a plane distribution that is not tangent to a surface on any open subset of Y. A plane field can locally be given as the kernel of a 1–form $\alpha \in \Omega^1(Y)$, then the Frobenius Theorem translates to these settings; the plane field is integrable if and only if $\alpha \wedge d\alpha$ vanishes. If $\alpha \wedge d\alpha$ is nowhere 0, then $\xi = \ker \alpha$ is non-integrable. The contact structure is cooriented if ξ can be globally given as $\ker \alpha$. The plane field ξ is called positive, if the 3–form $\alpha \wedge d\alpha$ provides a volume-form for the oriented 3–manifold Y. In the following we will only deal with positive cooriented contact structures, and will simply refer to them as contact structures. Two contact 3–manifolds (Y_1, ξ_1) and (Y_2, ξ_2) are *contactomorphic* if there is a diffeomorphism $f\colon Y_1 \to Y_2$ with $f_*(\xi_1) = \xi_2$. Two contact structures ξ_1 and ξ_2 on the same 3–manifold Y are said to be *isotopic* if there is a contactomorphism $f\colon (Y, \xi_1) \to (Y, \xi_2)$ isotopic to the identity. The standard contact structure ξ_{st} on $\mathbb{R}^3$ (or on S^3) is given as the kernel of the 1–form $\alpha_{\text{st}} = dz + xdy$. A visualization of the contact plane fields is given on Figure 7. Contact structures are

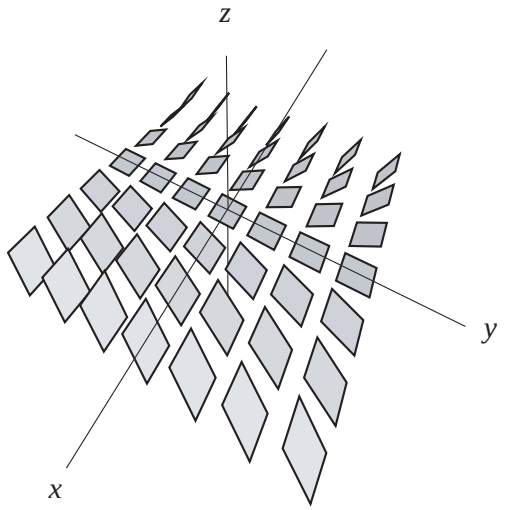

Figure 7. The standard contact structure on S^3. (Figure courtesy of S. Schönenberger.)

determined in the neighborhood of compact sets:

Theorem 3.1 (Moser's method)**.** *Let Z be a compact subspace of a closed oriented 3–manifold Y. Suppose, that there are two contact structures ξ_1 and ξ_2 given on Y that coincide when restricted to Z. Then there is a neighborhood U of Z such that $\xi_1|_U$ and $\xi_2|_U$ are isotopic contact structures relative Z.*

In particular every contact 3–manifold locally looks like this standard one. Using cylindrical coordinates another contact structure on $\mathbb{R}^3$ (or on S^3) can be defined as $\xi_{\text{OT}} = \ker(\cos r\, dz + r \sin r\, d\vartheta)$. (See Figure 8.) Both ξ_{st} and ξ_{OT} rotate in a clockwise

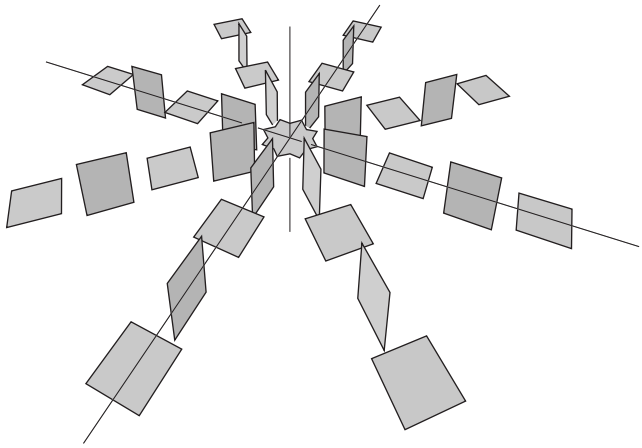

FIGURE 8. An overtwisted contact structure ξ_{OT} on S^3. (Figure courtesy of S. Schönenberger.)

manner as we move along the z axis, but while ξ_{st} only makes one twist ξ_{OT} makes several. This latter property of a contact structure is called overtwistedness. A precise definition of it goes as follows. An *overtwisted disc* is a disc with the contact planes being tangent to it along its boundary. For example the disc $D^2 = \{(0, \theta, r) : r \leq \pi\}$ in (S^3, ξ_{OT}) is an overtwisted disc. Contact structures containing overtwisted discs are called *overtwisted* contact structures, the ones with no overtwisted discs are *tight* contact structures. By a fundamental theorem of Eliashberg [5] on a given 3–manifold the isotopy classes of overtwisted contact structures can be classified in terms of only homotopical properties; two contact structures are isotopic if the corresponding plane fields are homotopic. The classification of tight contact structures is more stubble and have only been determined for a few 3–manifolds; S^3, lens spaces, circle bundles, torus bundles and some special Seifert fibred 3-manifolds. Another class of contact structures can be given on $T^2 \times I$. The contact structure ξ_n on $T^2 \times [0,1] = \mathbb{R}/\mathbb{Z} \times \mathbb{R}/\mathbb{Z} \times [0,1] =$

$\{(x,y,z)\}$ is defined by $\xi_n = \ker(\cos(2\pi nz)dx - \sin(2\pi nz)dy)$. A (not necessarily closed) contact 3–manifold (Y,ξ) has *Giroux torsion* $\tau(Y,\xi) \geq n$ if it contains an embedded submanifold $T^2 \times I$ with the property that $(T^2 \times I, \xi|_{T^2\times I})$ is contactomorphic to $(T^2 \times [0,1], \xi_n)$. Overtwisted contact structures have Giroux torsion $\tau = \infty$.

The classification of tight contact structures led to the examination of its submanifolds that somehow respect the contact structure. We will first describe special 1 dimensional and then 1 codimensional submanifolds.

3.1. **Legendrian and transverse knots.** There are two distinguished knot types in a contact structure (Y,ξ). A knot L in a closed, contact 3–manifold (Y,ξ) is *Legendrian* if the tangent vectors of the knot are contained by the contact 2–plane field ξ. The knot T is *transverse*, if the (nonzero) tangent vectors are nowhere contained by ξ. The coorientation of ξ endows transverse knots with an orientation. An application of Moser's method for Legendrian and transverse knots provides that these knots have standard neighborhoods.

By pushing off a Legendrian knot L in a direction transverse to ξ we obtain a transverse knot, the *transverse push off* of L. The push off inherits an orientation from L and we require this orientation to agree with the natural transverse orientation. As it can be seen from the sample local picture, a transverse knot T has Legendrian knots in its neighborhood, these knots are the *Legendrian approximations* of T. The transverse push off of a Legendrian approximation of T is T itself. As it will be explained later, transverse knots can be described as the equivalence classes of their Legendrian approximations.

Two Legendrian (transverse) knots are *Legendrian (transverse) isotopic* if they are isotopic through Legendrian (transverse) knots. Similarly to the smooth case these isotopies can be extended to the ambient 3–manifold. This equivalence relation is finer than the one given by smooth isotopy. One way to see that is by introducing new invariants. There are two classical invariants for null-homologous Legendrian knots defined as follows. By pushing off the knot in a transverse direction we obtain the *Thurston-Bennequin framing* of the Legendrian knot. Comparing this to the Seifert framing we get the *Thurston-Bennequin number* $\mathrm{tb}(L)$. The *rotation number* $\mathrm{rot}(L)$ is the winding number of TL with respect to a trivialization of the contact planes along L that extends to a Seifert surface. By pushing off the transverse knot T in a direction of a vector field in the contact planes that extends to a nonzero vector field to a Seifert-surface of

T we get T'. The *self-linking number* $\mathrm{sl}(T)$ is the linking of T with its push-off T'. An easy way to construct non-Legendrian (non-transverse) isotopic Legendrian knots is the stabilization of the knot. This is a local operation, thus it is sufficient to describe it only in the standard contact 3–sphere which we will do in the next Subsection. Once the Legendrian knot is oriented there are two types of stabilizations: positive and negative producing L_+ and L_- from L. These operations change the invariants: $\mathrm{tb}(L_\pm) = \mathrm{tb}(L) - 1$ and $\mathrm{rot}(L_\pm) = \mathrm{rot}(L) \mp 1$. For transverse knots there is only one stabilization corresponding to the positive stabilization of the Legendrian knots in its neighborhood. Stabilization gives a nice relation between Legendrian approximations of a transverse knot T giving rise to an alternate description of transverse isotopy. Two transverse knots are transversely isotopic if and only if their Legendrian approximations have common negative stabilizations. This allows us to mainly deal with Legendrian knots. The self-linking number of a transverse knot T can be deduced from the classical invariants of its Legendrian approximation L: $\mathrm{sl}(L) = \mathrm{tb}(L) - \mathrm{r}(L)$. Note that this value is independent of the chosen Legendrian approximation. Sometimes the classical invariants are enough to tell Legendrian (transverse) realizations of a knot-type apart; a knot is called *Legendrian simple* (or *transversely simple*) if any two Legendrian (transverse) realizations of it with equal Thurston-Bennequin and rotation (self-linking) number(s) are isotopic through Legendrian (transverse) knots.

3.2. **Knots in the standard contact space and front projections.** Recall that a *Legendrian knot* L in $\mathbb{R}^3$ (or in $S^3 = \mathbb{R}^3 \cup \{\infty\}$) endowed with the standard contact form $dz + xdy$ is an oriented knot along which the form $dz + xdy$ vanishes identically. Thus Legendrian knots are determined by their front projection to the yz-plane; a generic projection is smooth in all but finitely many cusp points, has no vertical tangents and at each crossing the strand with smaller slope is in the front. By changing the parts with vertical tangents to cusps and adding zig-zags, a generic smooth projection of a knot can be arranged to be of the above type. Thus any knot can be placed in Legendrian position. (Figure 24 depicts a Legendrian realization of the righthanded trefoil knot.) But this can be done in many different ways up to Legendrian isotopy. For example, by adding extra zig-zags in the front projection we obtain a different Legendrian representative. Figure 10 depicts the operation of adding a downward (upward) cusp. This method is called positive (negative) stabilization, see Figure 10.

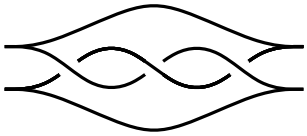

FIGURE 9. Righthanded trefoil knot

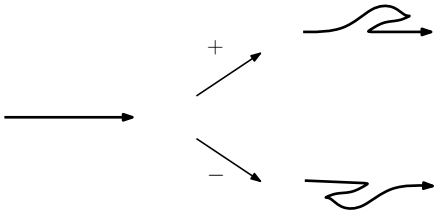

FIGURE 10. Positive and negative stabilization.

As in the smooth case, Legendrian isotopy can be understood in terms of the front projection; two front projections correspond to Legendrian isotopic Legendrian knots if they are related by a finite sequence of Legendrian Reidemeister moves of Figure 11.

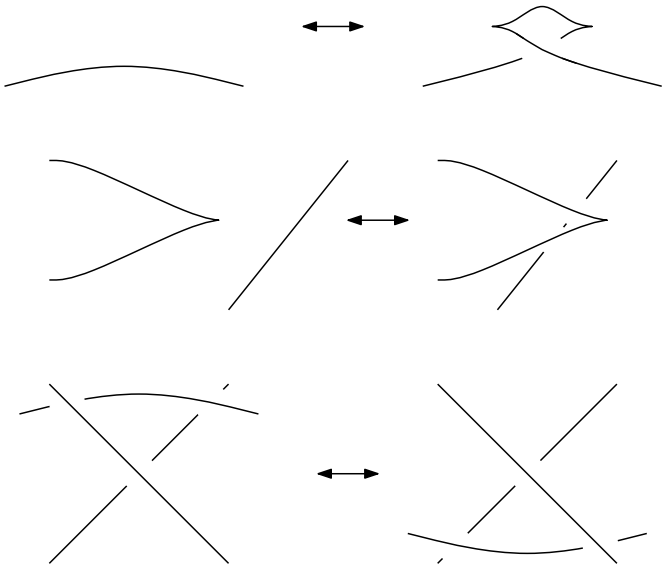

FIGURE 11. Legendrian Reidemeister moves

The connected sum of knots were defined by using an arc connecting them. The ambiguity of the connected sum operation is even more apparent in to Legendrian

case, as a fixed connecting arc can have many Legendrian representatives. Similarly to the smooth case in the standard contact 3–sphere there is a way around it. As it is described in [15] we can think of the two knots, as sitting in two disjoint standard contact 3–spheres, and we can connect sum the two spheres using a small ball in which the Legendrian arcs are standard. Figure 12 depicts the effect of the above process in the front projection.

3.3. **Convex surface theory.** On a generic (not necessarily closed) surface Σ in a contact structure (Y, ξ) the linefield $\xi \cap T\Sigma$ defines a singular foliation of Σ with isolated elliptic or hyperbolic singularities. In a nonsingular point the foliation can be oriented as follows. Pick a normal vector n coorienting ξ in $T\Sigma$, then the vector $v \in \xi \cap T\Sigma$ orients the foliation if (v, n) forms a positive basis of $T\Sigma$. The sign of a singular point is positive if the orientation of $T\Sigma$ and ξ coincide and negative otherwise. With this choice of orientation positive elliptic points become sources and negative elliptic points become sinks. The above described singular foliation is called the characteristic foliation of the surface Σ and is denoted by $\mathcal{F}_\Sigma$. The characteristic foliation determines the contact structure on the surface, thus by Moser's method it also determines it in the neighborhood of the surface. As an example, study the characteristic foliation on the overtwisted disc $D^2 = \{(0, \theta, r) : r \leq \pi\}$ in (S^3, ξ_{OT}). As it is shown on the left hand side of Figure 13, it has singularities along its boundary and in the origin. To put it into generic position we can slightly push its middle up fixing only its boundary. The obtained characteristic foliation is as shown on the right hand side of Figure 13 has only one elliptic singular point.

As it was observed by Giroux [21] for a special but still dense class of surfaces called convex surfaces even less structure -a multicurve- is enough to describe the contact

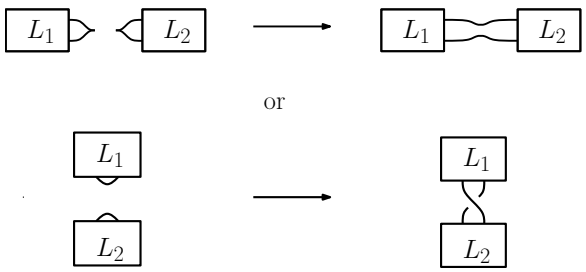

FIGURE 12. Connected sum of two Legendrian knots.

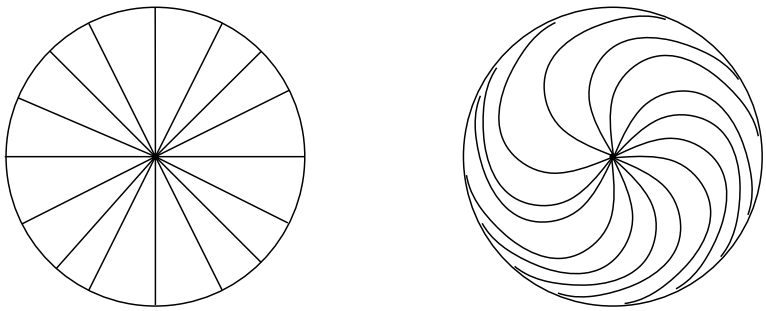

FIGURE 13. Characteristic foliation on an overtwisted disc.

structure in a neighborhood of the surface. So it is easy to glue contact structures along convex surfaces, thus this will be the boundary condition for contact 3–manifolds with boundary. A *contact vector field* v on a contact 3–manifold is a vector field whose flow preserves the contact structure. A surface Σ is convex, if there is a contact vector field (positively) transverse to it. In the case when Σ is not closed we also require its boundary to be Legendrian. Giroux's theorem [21] states that any closed surface is C^∞-close to a convex surface, and according to Kanda [7] a surface with Legendrian boundary can also be C^∞–perturbed fixing the boundary to a convex surface provided all of its boundary components have negative Thurston-Bennequin numbers. The set $\Gamma_\Sigma = \{x : v \in \xi\}$ defines a multicurve (a properly embedded 1-manifold) in Σ whose isotopy-class is independent of the chosen contact vector field. The dividing curve Γ divides Σ into two parts $\Sigma_+ = \{x : \alpha(v) > 0\}$ and $\Sigma_+ = \{x : \alpha(v) < 0\}$. By Giroux [21] the isotopy class of Γ determines the contact structure in a neighborhood of the convex surface. If the surface S is a Seifert surface for a Legendrian knot L, than the definition of the rotation number translates to $\mathrm{r}(L) = \chi(S_+) - \chi(S_-)$. If the Legendrian knot has negative Thurston-Bennequin number then it can be read off from the dividing curves as $\mathrm{tb}(L) = -\frac{1}{2}|\Gamma_S \cap L|$. The dividing curve of the overtwisted disc $D^2 = \{(0, \theta, r) : r \leq 1\}$ in (S^3, ξ_{OT}) is a closed curve around the elliptic point.

3.4. **Bypass attachment.** If we isotope a convex surface Σ in a contact 3-manifold, then the isotopy class of the dividing curve does not change as long as the contact vector field is transverse to Σ. The change the isotopy class Γ_Σ experiences once the contact vector field fails to be transverse to Σ is called *bypass attachment*. For a complete discussion of bypass attachments see [23]. Let $(Y, \partial Y, \xi)$ be a contact 3–manifold with convex boundary. Suppose that we are given a Legendrian arc $c \subset \partial Y$ that starts and

ends on the dividing set $\Gamma_{\partial Y}$ and intersects $\Gamma_{\partial Y}$ in one additional point. Attaching a *bypass* along c is — roughly speaking — the attachment of the neighborhood of a "half overtwisted disc". This is a disc D with boundary $\partial D = c \cup d$, where $\partial D \cap \partial Y = c$, and the dividing curve on D consists of a single arc with both of its endpoints on c. The resulting manifold is diffeomorphic to Y with contact structure ξ^c, and the dividing curve Γ is changed in the neighborhood of c to Γ^c as it is shown on Figure 14.

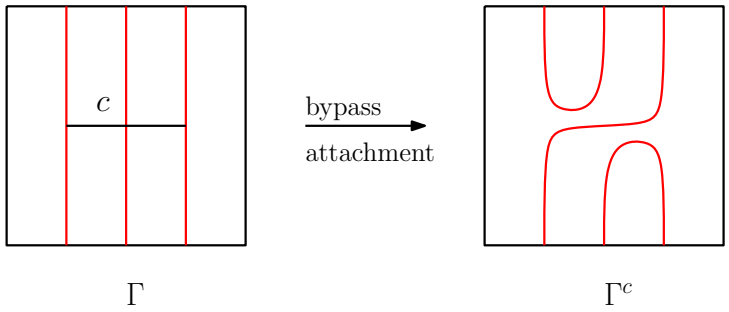

FIGURE 14. Bypass attachment.

It was already known [6], that there is a unique tight contact 3-ball. Using convex surface theory, classification of tight contact structures was done on certain 3–manifolds. Basic slices are the building blocks for contact structures on $T^2 \times I$.

We give a short description of basic slices defined by Honda [23]. Suppose that ξ is a contact structure on $T^2 \times [0,1]$ with convex boundary with two–component dividing curves on each of its boundary components. The dividing curves are homotopically nontrivial and parallel curves. Fix a trivialization for T^2 as $\mathbb{R}^2/\mathbb{Z}^2$ and let s_i denote the slope of the dividing curves on $T^2 \times \{i\}$ $(i \in \{0,1\})$. The contact 3–manifold $(T^2 \times [0,1], \xi)$ is called *minimally twisting* if every convex torus parallel to the boundary has slope s in $[s_1, s_0]$. (Here by $[s_1, s_0]$ we mean $[s_1, \infty] \cup [-\infty, s_0]$ if $s_1 \geq s_0$.) A *basic slice* is a minimally twisting tight contact structure $(T^2 \times [0,1], \xi)$, with convex boundary and with two dividing curves on each $T^2 \times \{i\}$ and boundary slopes s_0 and s_1 forming an integral basis for $\mathbb{Z}^2$. For fixed boundary conditions (up to isotopy) there are two basic slices distinguished by their relative Euler class, which differ only by their sign. Note that there is no canonical positive or negative choice.

One way to obtain a basic slice is by gluing a bypass to an I–invariant neighborhood of a convex T^2 with two dividing curves. For a given slope of the attaching curve there

are two ways of attaching a bypass corresponding to the two different basic slices, cf. Figure 17. Any basic slice can be obtained by this construction.

Suppose that $(T^2\times[0,1],\xi_0)$ and $(T^2\times[1,2],\xi_1)$ are basic slices with boundary slopes s_i on $T^2\times\{i\}$ $(i\in\{0,1,2\})$. As the dividing curves match up on $T^2\times\{1\}$, we can glue them together to obtain $(T^2\times[0,2],\xi=\xi_0\cup\xi_1)$. If in addition we require that the shortest representatives of s_0 and s_2 give an integral basis for $\mathbb{Z}^2$ and $[s_0,s_1]\cup[s_1,s_2]\neq[-\infty,\infty]$, then $(T^2\times[0,2],\xi)$ is minimally twisting. It is either overtwisted or a single basic slice depending on whether the basic slices $(T^2\times[0,1],\xi_0)$ and $(T^2\times[1,2],\xi_1)$ have the same or opposite signs. Note, that "having the same sign" makes sense in this setting, once we require the trivialization of ξ_0 and ξ_1 to agree over $T^2\times\{1\}$.

3.5. **Open book decompositions.** Giroux [22] found a one-to-one correspondence between isotopy classes of contact structures and open book decompositions up to positive stabilization/destabilization on a closed oriented 3-manifold. An *open book decomposition* of a 3–manifold Y is a fibration of $Y-B$ over S^1, where B is a 1–dimensional submanifold such that the boundary of each fiber $\mathring{S}$ is B. In this context the closure of the fiber S is called a *page* and the 1-manifold B is called the *binding* of the open book. The fibration can be descried by its monodromy $g\colon S\to S$. From a pair (S,g) the 3–manifold Y can be rebuilt as $Y=S\times[-1,1]/\sim$, where $\sim$ is defined as $(x,t)\sim(x,t')$ for $x\in\partial S$ and $t,t'\in[-1,1]$, and $(x,-1)\sim(g(x),1)$. This pair (S,g) is an *abstract open book* defining Y. Open book decompositions not only describe 3–manifolds but a contact structure can be naturally associated to them as follows. The 3–manifold Y decomposes to two handlebodies $U_\beta=S\times[-\frac{1}{2},\frac{1}{2}]$ and $U_\alpha=S\times([\frac{1}{2},1]\cup[-1,-\frac{1}{2}])$. Using convex surface theory Torisu showed [50] that on the handlebodies U_α and U_β there is a unique tight contact structure with dividing curves ∂S. Gluing these tight contact structures together we obtain a contact structure ξ on Y. In the above case (S,g) is said to support the contact structure ξ. For example S^3 has an open book decomposition with binding $B=\{(x,0,0)\}$ and pages $S_\theta=\{(x,\sin\theta,\cos\theta)\}$. The corresponding abstract open book has disc pages $(S=D^2)$ and trivial monodromy. The two handlebodies are balls with the unique tight contact structure, and after gluing them together we obtain the standard contact 3–sphere. The proof that any closed contact 3–manifold (Y,ξ) has an open book decomposition supporting it uses contact cell-decompositions. A *contact cell-decomposition* of a contact 3–manifold is a cell decomposition, whose 1–skeleton is a Legendrian graph, 2–discs are convex with $\mathrm{tb}=-1$ boundaries, and the

3–cells are standard contact 3-balls. Now the neighborhood of the 1–skeleton can be written as $\nu(\mathrm{sk}_1) = S \times [0,1]/\sim$, where $S = (-\partial(\nu(\mathrm{sk}_1)))_+$, and as the remaining part is a neighborhood of the dual Legendrian graph with the same boundary, we can write it as $Y - \nu(\mathrm{sk}_1) = S \times [0,1]/\sim$. The monodromy g can be read off from the gluing of the two handlebodies, giving an abstract open book decomposition (S, g) supporting (Y, ξ). Introducing a new edge in the 1-skeleton changes the abstract open book in a well understood way, which we call the *positive stabilization* of the open book. A positive stabilization of an open book supports the same contact structure. Giroux's observation [22] is that the converse statement is true: two abstract open books support isotopic contact structures if and only if they have common positive stabilizations.

3.6. **3–manifolds with boundary and partial open book decompositions.** Partial open books are generalizations of open books for 3–manifolds with convex boundary. This notion was introduced by Honda, Kazez and Matić in [24], see also [10, 11].

Definition 3.2. An *abstract partial open book* is a triple (S, P, h) where S is a connected surface with boundary, P is a proper subsurface of S which is a union of 1–handles attached to $S - P$, and $h\colon P \to S$ is an embedding that restricts to the identity near the boundary $\partial P \cap \partial S$.

A partial open book defines a 3–manifold Y with boundary as follows. First construct the handlebody $S \times [-1,0]/\sim$ and the compression–body $P \times [0,1]/\sim$, where $(x,t) \sim (x,t')$ for $x \in \partial S$ and $t, t' \in [-1,1]$. (Note that on $P \times [0,1]$ we just contract the points with first coordinate in $\partial P \cap \partial S$.) Then glue them together with the maps $P \times \{0\} \hookrightarrow S \times \{0\}$ and $h\colon P \times \{1\} \to S \times \{-1\}$. A schematic picture for Y is given by Figure 15. The resulting 3–manifold naturally carries the structure of a balanced sutured manifold: take $\Gamma = \overline{\partial S - \partial P} \times \{-\frac{1}{2}\} \cup -\overline{(\partial P - \partial S)} \times \{\frac{1}{2}\} \subset \partial Y$. Now $R_+ = \overline{S - P} \times \{0\}$, $R_- = \overline{S - h(P)} \times \{-1\}$, consequently $\chi(R_+) = \chi(R_-)$ follows at once.

Both the handlebody $S \times [-1,0]/\sim$ and the compression–body $P \times [0,1]/\sim$ admit unique tight contact structures with convex boundary and dividing set ∂S (and ∂P, resp), cf. [11, 50]. As the dividing sets match up, we can glue these contact structures to obtain a contact structure ξ on Y with dividing curve Γ on the convex boundary ∂Y. In this sense a partial open book decomposition determines a contact structure with convex boundary.

The partial open book decomposition naturally induces a balanced Heegaard decomposition of Y with the compression bodies $U_\alpha = P \times [\frac{1}{2}, 1] \cup S \times [-1, -\frac{1}{2}]$ and $U_\beta = S \times [-\frac{1}{2}, 0] \cup P \times [0, \frac{1}{2}]$, divided by the Heegaard surface $\Sigma = \partial U_\alpha = S \times \{-\frac{1}{2}\} \cup -P \times \{\frac{1}{2}\}$. Consistently with the sutured 3–manifold structure, the boundary of U_α (and U_β, resp.) consists of the union of Σ (resp. $-\Sigma$), R_- (resp. R_+) and a collar neighborhood for Γ; furthermore $\Gamma = \partial\Sigma (= \partial R_+ = -\partial R_-)$. Note that the dividing curve on ∂Y induced by the partial open book decomposition, and the sutures of the sutured decomposition coincide and both is denoted by Γ.

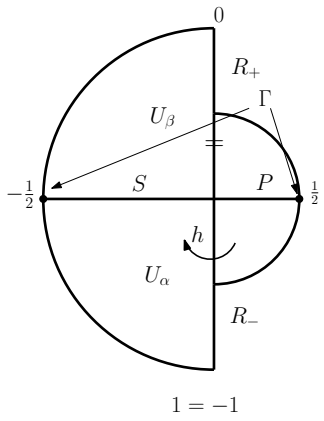

FIGURE 15. Schematic picture of a partial open book decomposition.

Every contact 3–manifold with convex boundary (Y, ξ) admits a partial open book decomposition that is compatible with ξ in the above sense, cf. [24]. To see this, consider a contact cell–decomposition for Y whose 1–skeleton C is a direct product near the boundary ∂Y and intersects the boundary on the dividing curves. As Legendrian arcs have standard neighborhood, there is a small neighborhood $\nu(C)$ of C with convex boundary and with a dividing curves of two components. The dividing curve separates $-\partial\nu(C)$ into a positive and a negative part $(-\partial\nu(C))_+$ and $(-\partial\nu(C))_-$. Setting $P = (-\partial\nu(C))_+$ the neighborhood $\nu(C)$ can be written as $P \times [0, 1]/\sim$. As C was the 1–skeleton of a contact cell decomposition, $Y - \nu(C)$ is product disc–decomposable: it is divided by the 2–cells (that are discs with $\mathrm{tb} = -1$) to a union of tight contact 3–balls. Thus for $S = \partial(Y - \nu(C))_+$ the handlebody $Y - \nu(C)$ can be written as $Y - \nu(C) = S \times [-1, 0]/\sim$, and $P = (-\partial(\nu(C)))_+ \subseteq (\partial(Y - \nu(C)))_+ = S$. Note that

by construction $\xi|_{Y-\nu(C)}$ is tight, its boundary $\partial(Y-\nu(C))$ is convex, and the dividing set $\Gamma_{\partial(Y-\nu(C))}$ is isotopic to $\partial S \times \{0\}$.

4. Invariants for Legendrian and transverse knots

Heegaard Floer homology provided various sets of invariants: for knots in the standard contact 3–sphere the combinatorial construction of knot Floer homology through grid diagrams [35, 45], for null–homologous knots in general contact 3–manifolds the Legendrian invariant of [30] and for general Legendrian knots the sutured invariant of the knot complement [24]. One aim of this dissertation is to set up a relation between these last two invariants.

4.1. **Legendrian and transverse invariants on grid diagrams.** Consider a grid diagram G. It describes not only a knot projection but also a front projection of a Legendrian realization of its mirror $m(K)$, as follows. Rotate the grid diagram by 45° clockwise, reverse the over- and under crossings and turn the corners into cusps or smooth them as appropriate. Legendrian Reidemeister moves correspond to certain grid moves giving the following result:

Proposition 4.1. *(Ozsváth–Szabó–Thurston,* [45]*) Two grid diagrams represent the same Legendrian knot if and only if they can be connected by a sequence of cyclic permutation, commutation, and (de)stabilization of types $X:NW$, $X:SE$, $O:NW$ and $O:SE$.* □

Moreover stabilizations of type $X:NE$ or $O:SW$ of the grid diagram correspond to negative stabilization of the knot, yielding

Proposition 4.2. *(Ozsváth–Szabó–Thurston,* [45]*) Two grid diagram represent the same transverse knot if and only if they can be connected by a sequence of cyclic permutation, commutation, and (de)stabilization of types $X:NW$, $X:SE$, $X:NE$, $O:NW$, $O:SE$ and $O:SW$.* □

Consider a grid diagram G for a Legendrian knot L of knot type K. Pick the upper right corner of every cell containing an X. This gives a generator of $CFK^-(m(K))$ denoted by $\mathbf{x}_+(G)$. Since positive rectangles starting at $\mathbf{x}_+(G)$ must intersect some X, the element $\mathbf{x}_+(G)$ is a cycle defining an element $\lambda_+(G)$ in $\mathrm{HFK}^-(m(K))$. Similarly one can define $\mathbf{x}_-(G)$ and $\lambda_-(G)$ by taking the lower left corners of the cells containing X's. These elements are proved to be independent of the grid moves that preserve the Legendrian knot type, giving an invariant of the Legendrian knot L:

Theorem 4.3. *(Ozsváth–Szabó–Thurston, [45]) Consider two grid diagrams G_1 and G_2 defining the same oriented Legendrian knot. Then there is a quasi-isomorphism of the graded chain complexes CFK^- taking $\mathbf{x}_+(G_1)$ to $\mathbf{x}_+(G_2)$ and $\mathbf{x}_-(G_1)$ to $\mathbf{x}_-(G_2)$.* □

One can understand the transformation of $\mathbf{x}_+(G)$ and $\mathbf{x}_-(G)$ under positive and negative stabilization:

Theorem 4.4. *(Ozsváth–Szabó–Thurston, [45]) Let L be an oriented Legendrian knot, denote by L_+ its positive and by L_- its negative stabilization. Then*

(1) *There is a quasi-isomorphism of the corresponding graded complexes taking $\mathbf{x}_+(L)$ to $\mathbf{x}_+(L_+)$ and $U\mathbf{x}_-(L)$ to $\mathbf{x}_-(L_+)$;*
(2) *There is a quasi-isomorphism of the corresponding graded complexes taking $U\mathbf{x}_+(L)$ to $\mathbf{x}_+(L_-)$ and $\mathbf{x}_-(L)$ to $\mathbf{x}_-(L_-)$.*

□

It follows from [14] that the Legendrian knots with transversely isotopic positive push offs admit common negative stabilizations. This principle provides a well defined invariant for transverse knots: if L is a Legendrian approximation of T then define $\theta(T) = \lambda_+(L)$.

Theorem 4.5. *(Ozsváth–Szabó–Thurston, [45]) For any two grid diagrams G_1 and G_2 of Legendrian approximations of the transverse knot T there is a quasi-isomorphism of the corresponding graded chain complexes inducing a map on the homologies that takes $\theta(G_1)$ to $\theta(G_2)$.* □

4.2. **The contact invariant for 3–manifolds with boundary.** Suppose that (Y, ξ) is a contact 3–manifold with convex boundary, and consider a partial open book compatible with ξ. Let $\{b_1, \dots, b_k\}$ be disjoint arcs forming a basis for $H_1(P, \partial S \cap \partial P)$. The disks swept out by the b_i's in the U_β handlebody have boundaries $\beta_i = b_i \times \{\frac{1}{2}\} \cup b_i \times \{-\frac{1}{2}\}$. Isotope each b_i to an arc a_i that intersects it transversely in a single point, and whose endpoints are moved in the direction given by the boundary orientation of $-P$. In the U_α handlebody a_i sweeps out a disk with boundary $\alpha_i = a_i \times \{\frac{1}{2}\} \cup h(a_i) \times \{-\frac{1}{2}\}$, providing a Heegaard diagram $(\Sigma, \boldsymbol{\alpha}, \boldsymbol{\beta})$ for (Y, Γ). The single intersection point $\mathbf{y} = (a_i \cap b_i)$ on $P \times \{\frac{1}{2}\}$ can be shown to represent a cycle in $\mathrm{SFC}(-\Sigma, \boldsymbol{\alpha}, \boldsymbol{\beta})$, thus it defines an element $\mathrm{EH}(Y, \xi)$ in $\mathrm{SFH}(-Y, -\Gamma)$. (Notice the reversal of orientation of the Heegaard surface Σ.) As has been proven by Honda, Kazez and Matić [24], this element is independent

of the choices made throughout its definition and gives the invariant $\mathrm{EH}(Y,\xi)$ of the contact structure (Y,ξ). In the special case when the contact 3–manifold with convex boundary is given as the complement of a standard neighborhood of a Legendrian knot in a closed contact 3–manifold (Y,ξ), the resulting element will be denoted by $\mathrm{EH}(L)$. Note that by the Legendrian Neighborhood Theorem, in this case Γ consists of two parallel simple closed curves in $\partial(Y-\nu(L))$.

4.3. **Legendrian and transverse invariants in arbitrary 3–manifolds.** Consider an oriented, null–homologous Legendrian knot in the closed contact 3–manifold (Y,ξ). There is an open book decomposition of Y compatible with ξ containing L homologically essentially on one of its pages $S = S\times\{\frac{1}{2}\}$. Consider a properly embedded arc b_1 in S intersecting L exactly once. The disk $b_1\times[0,1]$ is a meridional disk for L. Orient b_1 so that the boundary orientation of $\partial(b_1\times[0,1]) = -b_1\times\{0\}\cup b_1\times\{1\}$ agrees with the natural orientation of the meridian for L. (Such an oriented arc b_1 will be called a *half–meridian* of L.) With these conventions the orientation of S coincides with the orientation induced by (b_1,L). Our setup here will be slightly different from the one used in [30], but the resulting Heegaard diagram and the element specified in it will be actually the same already on the chain–level.

Pick a basis $\{b_1,\dots,b_g\}$ of $H_1(S,\partial S)$ such that b_1 is a half–meridian of L. Isotope all the b_i's to a_i's as before and place the basepoint z in the "big" region that is not swept out by the isotopies of the b_i, and put w between b_1 and a_1. This can be done in two essentially different ways, and exactly one of them corresponds to the chosen orientation of L. If b_1 is oriented as described above, w should be placed close to the tail of b_1, cf. Figure 16. The single intersection point $(a_i\cap b_i)$ on $S\times\{\frac{1}{2}\}\subset -\Sigma$ is an

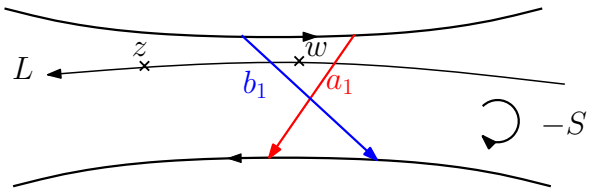

FIGURE 16. The placement of the basepoints.

element in $\widehat{\mathrm{CFK}}(-\Sigma,\boldsymbol{\alpha},\boldsymbol{\beta},z,w)$ and the choice of z assures that it is a cycle, hence it defines an element $\widehat{\mathcal{L}}(L)$ in $\widehat{\mathrm{HFK}}(-Y,L)$. As it was shown in [30], the homology class $\widehat{\mathcal{L}}(L)$ is an invariant of the oriented Legendrian knot $L\subset(Y,\xi)$.

5. Relation between the invariants

In this section we will set up a relation between the last two invariants. To set the stage, recall that the Legendrian invariant $\widehat{\mathcal{L}}(L)$ of the null–homologous Legendrian knot $L \subset (Y, \xi)$ defined in [30] takes its value in the knot Floer homology group $\widehat{\mathrm{HFK}}(-Y, L)$. (The theory admits a version where the invariants are in the more refined group $\mathrm{HFK}^-(-Y, L)$, but since the corresponding sutured theory is not developed yet, we will deal only with the $\widehat{\mathrm{HFK}}$–version.) A relation between sutured Floer homology and knot Floer homology obviously follows from their definitions: suppose that $(Y - \nu(L), \Gamma)$ is the sutured 3–manifold with toric boundary we get by deleting a neighborhood of the (not necessarily Legendrian) knot L and Γ has two (parallel) components. Then there is an obvious isomorphism

$$\Psi \colon \mathrm{SFH}(Y - \nu(L), \Gamma) \to \widehat{\mathrm{HFK}}(Y_\Gamma, L')$$

where Y_Γ is the Dehn filling of $Y - \nu(L)$ (and L' is the core of the Dehn filling) with slope given by the sutures Γ. In general, Y_Γ differs from Y (and therefore L' differs from L). By attaching a specific contact $T^2 \times [0, 1]$ (a *basic slice*) to $Y - \nu(L)$, the composition of the map

$$\Phi \colon \mathrm{SFH}(-(Y - \nu(L)), -\Gamma) \to \mathrm{SFH}(-(Y - \nu(L)), \Gamma')$$

of [25] induced by this attachment and the above map Ψ (applied to the suture Γ' with components isotopic to the meridian of the knot) gives a map

$$F \colon \mathrm{SFH}(-(Y - \nu(L)), -\Gamma) \to \widehat{\mathrm{HFK}}(-Y, L)$$

for which we show the following:

Theorem 5.1. *Fix an orientation on the Legendrian knot L and consider one of the basic slices with boundary slopes given by the dividing set of $\partial(Y - \nu(L))$ on $T^2 \times \{0\}$ and by the meridian of L on $T^2 \times \{1\}$. Then the map F defined above maps* $\mathrm{EH}(L)$ *to* $\widehat{\mathcal{L}}(L)$.

A more precise formulation of the theorem will be given in Section **??** after basic slices and orientations have been discussed. A straightforward consequence of the above relation is the following

Corollary 5.2. *If the complement of a null–homologous Legendrian knot has positive Giroux torsion then $\widehat{\mathcal{L}}(L)$ vanishes.*

Remark 5.3. The same corollary has been found recently by D. S. Vela–Vick [51] using slightly different arguments.

To put this result in perspective, we recall that a knot type in the standard contact 3–sphere is called *Legendrian simple* if two Legendrian knots of the given knot type and identical Thurston–Bennequin and rotation numbers (for definitions of these invariants see [14]) are Legendrian isotopic. The same notion generalizes to an arbitrary ambient contact 3–manifold (Y, ξ), with a caveat in the case when ξ is overtwisted: in that case Legendrian knots fall into two categories, depending on whether the knot complement is overtwisted (in which case the knot is called *loose*) or — although ξ is overtwisted — the knot complement is tight (in which case the knot is *non–loose* or *exceptional*, cf. [9]). Obviously a loose and a non–loose knot cannot be isotopic, hence in overtwisted contact 3–manifolds besides the equality of the Thurston–Bennequin and rotation numbers we also require the equality of the looseness of the two knots in defining simplicity. Non–simple non–loose knots in a variety of overtwisted contact structures have been found in [30]. There is, however, a simple way of constructing non–simple non–loose knots [12]: suppose that the knot complement contains an incompressible torus (e.g., the knot type is a satellite in S^3) and introduce Giroux torsion along the torus. Since this procedure does not change the homotopy type of the 2–plane field, and ξ is overtwisted by assumption (and overtwisted structures are classified by their homotopy type), after a suitable choice of the knot and the torus we get a Legendrian knot in the same contact 3–manifold with different tight complement. (The verification that the complement remains tight, and that the implementations of different Giroux torsions result in different structures requires delicate arguments [12].) This method, in fact, can produce infinitely many different Legendrian non–loose knots with the same numerical invariants in these knot types [12]. We say that $L \subset (Y, \xi)$ is *strongly non–loose* if ξ is overtwisted and the knot complement is tight with vanishing Giroux torsion. The knot type is *strongly non–simple* if there are two strongly non–loose, smoothly isotopic knots with equal numerical invariants which are not Legendrian isotopic. The same simplicity/non–simplicity definition (with the strong adjective) carries through verbatim for transverse knots (where the role of the numerical invariants is played by the

self–linking number of the transverse knot). In this sense, the result of [30] translates to

Corollary 5.4. *The knot types of* [30, Theorem 1.7 and Corollary 1.8] *are strongly non–simple.*

Proof. The distinction of the Legendrian knots L_i in [30] went by determining the Legendrian invariants $\widehat{\mathcal{L}}(L_i)$, and since both were nonzero, Corollary 5.2 implies that the knots L_i are strongly non–loose, concluding the proof. □

Notice that in [45] the combinatorial theory provided two invariants of L (denoted by $\widehat{\lambda}^{\pm}(L)$), while in [30] the invariant $\widehat{\mathcal{L}}(L)$ depended on an orientation of L — therefore an unoriented Legendrian knot admitted two invariants $\widehat{\mathcal{L}}(L)$ and $\widehat{\mathcal{L}}(-L)$ after an arbitrary orientation of L was fixed. On the other hand, the sutured theory provides a unique element for L. The discrepancy is resolved by the observation that the map on sutured Floer homology induced by the basic slice attachment is well–defined only up to a choice: with the given boundary slopes there are two basic slices, and using one transforms $\mathrm{EH}(L)$ into $\widehat{\mathcal{L}}(L)$, while with the other choice the result will be $\widehat{\mathcal{L}}(-L)$ (after an orientation on L is fixed). In order to clarify signs, we reprove a special case of [30, Theorem 7.2] (only in the $\widehat{\mathrm{HFK}}$–theory) regarding the effect of stabilization of L on $\widehat{\mathcal{L}}$ and show

Theorem 5.5. *Let L be an oriented null–homologous Legendrian knot. If L^- (and L^+) denotes its negative (resp. positive) stabilization, then $\widehat{\mathcal{L}}(L^-) = \widehat{\mathcal{L}}(L)$ and $\widehat{\mathcal{L}}(L^+) = 0$.*

Notice that the invariance of $\widehat{\mathcal{L}}$ under negative stabilization means that, in fact, it is an invariant of the transverse isotopy class of the positive transverse push–off of the Legendrian knot L. By this definition the extensions of Corollaries 5.2 and 5.4 to the transverse case are easy exercises. For further results regarding transverse knots using these invariants see [35, 37]. In fact, in [37] the distinction of various Legendrian and transverse Eliashberg–Chekanov (aka twist) knots and 2–bridge knots was carried out by computing their $\widehat{\mathcal{L}}$–invariants. As a corollary, Theorem 5.1 readily implies

Corollary 5.6. *The complement of the Eliashberg–Chekanov knot E_n (which is the 2–bridge knot of type $\frac{2n+1}{2}$) for odd n admits at least $\lceil \frac{n}{4} \rceil$ different tight contact structures (distinguished by the sutured invariant) with convex boundary and dividing set Γ of two components with slope 1.* □

Performing contact (-1)–surgery along a Legendrian knot L gives a well–defined contact structure ξ_{-1} on the surgered 3–manifold Y_{-1}. The core L' of the glued–back solid torus is a Legendrian knot in (Y_{-1}, ξ_{-1}). Suppose that L' is null–homologous in Y_{-1}. Using the sutured invariant we deduce

Theorem 5.7. *Under the circumstance described above* $\widehat{\mathcal{L}}(L) \neq 0$ *implies* $\widehat{\mathcal{L}}(L') \neq 0$.

5.1. **Proof of Theorem 5.1.** Let L be a Legendrian knot in a closed contact 3–manifold (Y, ξ). The two invariants $\mathrm{EH}(L) = \mathrm{EH}(Y - \nu(L), \xi|_{Y-\nu(L)}) \in \mathrm{SFH}(-(Y - \nu(L)), -\Gamma_{\partial(Y-\nu(L))})$ and $\widehat{\mathcal{L}}(L) \in \widehat{\mathrm{HFK}}(-Y, L)$ introduced above lie in two different groups, but if we change the suture on $\partial(Y - \nu(L))$ to two meridians $-m \cup m$ of L, the sutured Floer homology $\mathrm{SFH}(-(Y - \nu(L)), -m \cup m)$ can be identified with $\widehat{\mathrm{HFK}}(-Y, L)$. This modification of the suture can be achieved by attaching a basic slice to the sutured 3–manifold $Y - \nu(L)$, and according to [25] there is a map corresponding to this attachment. More generally:

Theorem 5.8 (Honda–Kazez–Matić, [25], cf. also [19])**.** *Suppose* (Y', Γ') *is a balanced sutured submanifold of the balanced sutured 3-manifold* (Y, Γ) *and all components of* $Y - int(Y')$ *intersect* ∂Y. *Let* ξ *be a contact structure on* $Y - int(Y')$ *so that* $\partial Y \cup \partial Y'$ *is convex with respect to* ξ *and with dividing set* $\Gamma \cup \Gamma'$. *Then there is a natural linear map*

$$\Phi_\xi \colon \mathrm{SFH}(-Y', -\Gamma') \to \mathrm{SFH}(-Y, -\Gamma),$$

induced by ξ. *Moreover, if* Y' *is endowed with the contact structure* ξ' *such that* $\Gamma_{(Y',\xi')} = \Gamma'$ *then*

$$\Phi_\xi(\mathrm{EH}(Y', \xi')) = \mathrm{EH}(Y, \xi' \cup \xi).$$

□

We will apply this theorem in the special case when $\partial Y'$ and ∂Y are both 2–tori, $Y - \mathrm{int}Y' = T^2 \times [0, 1]$ and the contact structure on the difference is a basic slice. The dividing set is given on $\partial(T^2 \times [0, 1])$ by the dividing set of ∂Y (on $T^2 \times \{0\}$) and by the meridians of L (on $T^2 \times \{1\}$); there are two basic slices with the given boundary slopes. Notice that the attachment of the basic slice is actually equivalent to the attachment of a single bypass.

Trivialize $\partial(Y - \nu(L))$ with the meridian m and the contact framing l, hence the dividing curves have slope ∞. The new dividing curve after attaching a bypass along any

arc with slope between -1 and 0 has slope 0. Up to isotopy there are only two different attachments (of opposite sign) depicted on Figure 17; these are the two different bypass attachments corresponding to the two different basic slices. These attaching curves together with the arcs of the dividing curves form an oriented curve on $\partial(Y-\nu(L))$, one of them represents m the other one represents $-m$. Denote the former one by c.

Theorem 5.9. *The map*

$$\Phi^c\colon \mathrm{SFH}(-(Y-\nu(L)),-\Gamma_{\partial(Y-\nu(L))}) \to \mathrm{SFH}(-(Y-\nu(L)),-m\cup m)$$

induced by the basic slice attachment along c maps $\mathrm{EH}(L)$ *to the class which is identified with* $\widehat{\mathcal{L}}(L)$ *under the identification*

$$\Psi\colon \mathrm{SFH}(-(Y-\nu(L)),-m\cup m) \to \widehat{\mathrm{HFK}}(-Y,L).$$

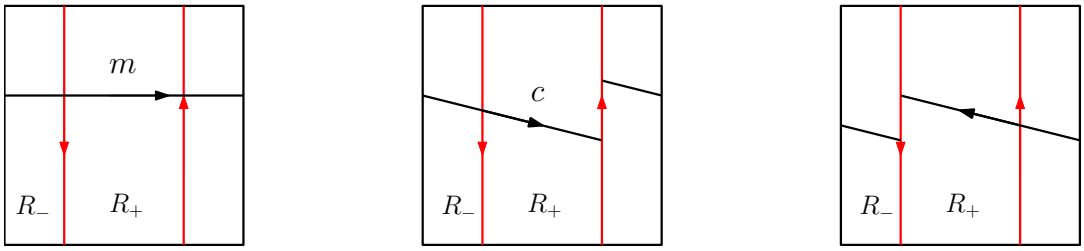

FIGURE 17. Bypass attachments to obtain meridians.

Proof. Let (S,g) be an open book for (Y,ξ) that contains L homologically essentially on one of its pages. Set $P=S-\nu_S(L)$ (where $\nu_S(L)$ denotes the tubular neighborhood of L in S) and $h=g|_P$. We claim that the partial open book (S,P,h) describes $(Y-\nu(L),\xi|_{Y-\nu(L)})$. Indeed, topologically the 3–manifold corresponding to this abstract partial open book is $(S\times[-1,0]/\sim)\cup(P\times[0,1]/\sim)$, which is equal to

$$(S\times[-1,1]/\sim)-(\nu_S(L)\times[0,1])=Y-\nu(L).$$

The contact structure on $S\times[-1,0]/\sim$ is the same, while on $P\times[0,1]/\sim$ (which is a subset of $S\times[0,1]/\sim$) it is obviously tight. If we round the corners we get that the dividing curve is $\Gamma_{\partial(Y-\nu(L))}$, so the dividing curve on $P\times[0,1]/\sim$ must be ∂P.

Take a basis $\{b_1,\dots,b_k\}$ of S subordinated to L, such that b_1 is the half–meridian of L. Then the left hand side of Figure 18 depicts the corresponding Heegaard diagram $(-\Sigma,\{\alpha_1,\dots,\alpha_k\},\{\beta_1,\dots,\beta_k\},w,z)$ for $(-Y,L)$. Here $\Sigma=S\times\{\frac{1}{2}\}\cup -S\times\{-\frac{1}{2}\}$

and the intersection point $\mathbf{x} = (a_i \cap b_i)_{i=1}^k$ represents the Legendrian invariant $\widehat{\mathcal{L}}(L)$ in $\widehat{\mathrm{HFK}}(-Y, L)$. The basis for $H_1(P, \partial S \cap \partial P)$ is $\{b_2, \dots, b_k\}$ while the Heegaard surface is $-\widetilde{\Sigma} = P \times \{\frac{1}{2}\} \cup -S \times \{-\frac{1}{2}\}$. The corresponding Heegaard diagram for $(-(Y - \nu(L)), -\Gamma_{\partial(Y-\nu(L))})$ is $(-\widetilde{\Sigma}, \{\alpha_2, \dots, \alpha_k\}, \{\beta_2, \dots, \beta_k\})$ which is depicted on the right hand side of Figure 18. By definition $\mathbf{y} = (a_i \cap b_i)_{i=2}^k$ represents the contact invariant $\mathrm{EH}(L) \in \mathrm{SFH}(-(Y - \nu(L)), -\Gamma_{\partial(Y-\nu(L))})$.

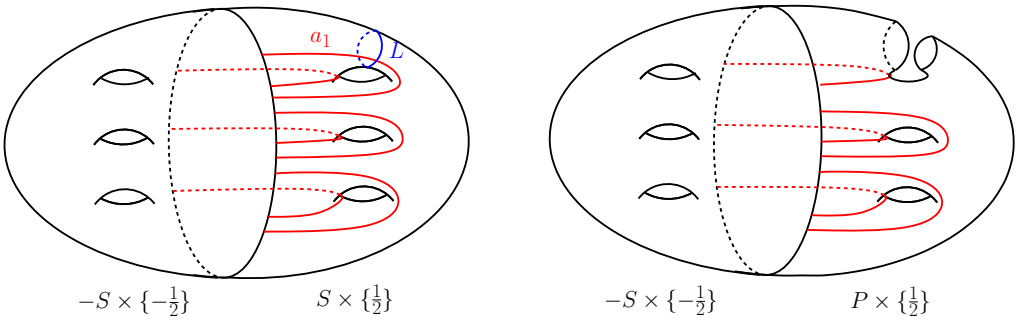

Heegaard diagram for Y Heegaard diagram for $Y - N(L)$

FIGURE 18. Heegaard diagrams corresponding to the (partial) open books.

Attaching a bypass along c changes the partial open book to (S', P', h'), where (with the notations described in Subsection 3.4) we have $S' = S \cup (1\text{–handle})$ and $P' = P \cup \nu(a_+)$. Note that a_+ represents half of the meridian on $(\partial(\nu(L)))_+ \subset S$, thus we can orient it. The 1–handle is attached to S along ∂S in the neighborhood of the head of a_+ so that both of its feet are in the positive direction away from the head of a_+ with respect to the orientation of ∂S, cf. Figure 19. The monodromy remains the same restricted to P (i.e. $h'|_P = h$) and as it was observed in Section 3.4, $h'(a_+) = a_-$ and a_- splits as the core of the 1–handle and as $a_- \cap S$ which is isotopic to c_-. Note that c_- is a half–meridian of the knot L, thus the image of it on $S \times \{-\frac{1}{2}\}$ is isotopic to $g(a_1)$. Now we are ready to describe the Heegaard diagram $(-(\Sigma', \{\alpha, \alpha'_2 \dots, \alpha'_k\}, \{\beta, \beta'_2, \dots, \beta'_k\}))$ obtained from the partial open book (S', P', h') in the usual manner. The Heegaard surface $-\Sigma'$ is equal to $P' \times \{\frac{1}{2}\} \cup -S' \times \{-\frac{1}{2}\}$, and the curves $\beta' = b_+ \times \{\frac{1}{2}\} \cup b_+ \times \{-\frac{1}{2}\}$ and $\alpha' = a_+ \times \{\frac{1}{2}\} \cup a_- \times \{-\frac{1}{2}\}$, where b_+ is the usual perturbation of a_+ on P'. Σ' is obtained by gluing two surfaces together, each of which is diffeomorphic to $S - \nu(\text{point})$. Indeed, the hole on the S'–side comes from the 1–handle attachment. P' is just a union of the 1–handles of S, thus the missing 2–handle gives us the other hole. This surface

Σ' is thus diffeomorphic to $\Sigma - \nu(z) - \nu(w)$, where we think of $\nu(z)$ being deleted from the S'–side and $\nu(w)$ from the P'–side. Under this identification b_+ (and thus a_+) is isotopic to b_1 on P', hence $\beta' = b_+ \times \{\frac{1}{2}\} \cup b_+ \times \{-\frac{1}{2}\}$ and β_1 are isotopic on Σ'. Recall that $h'(a_+)$ on $S' \times \{-\frac{1}{2}\}$ was isotopic to the union of $g(a_1)$ and the core of the 1–handle. So α' is isotopic to α_1 on $\Sigma - \nu(z)$. The core part of $h'(a_+)$ makes α' and β' to go around the hole $\nu(w)$ from different sides, thus α' is isotopic to α_1 on Σ'. In conclusion, the Heegaard diagram $(-\Sigma', \{\alpha', \alpha_2, \dots, \alpha_k\}, \{\beta', \beta_2, \dots, \beta_k\})$ is isotopic to $(-(\Sigma - \nu(z \cup w)), \{\alpha_1, \dots, \alpha_k\}, \{\beta_1, \dots, \beta_k\})$. The contact invariant $\mathrm{EH}(L)$ is mapped to the contact invariant $\mathrm{EH}(Y - \nu(L), -m \cup m)$ under the map induced by the basic slice attachment, and thus it represents the Legendrian invariant in $\widehat{\mathrm{CFK}}(-\Sigma, \boldsymbol{\alpha}, \boldsymbol{\beta}, z, w)$, which proves the statement. □

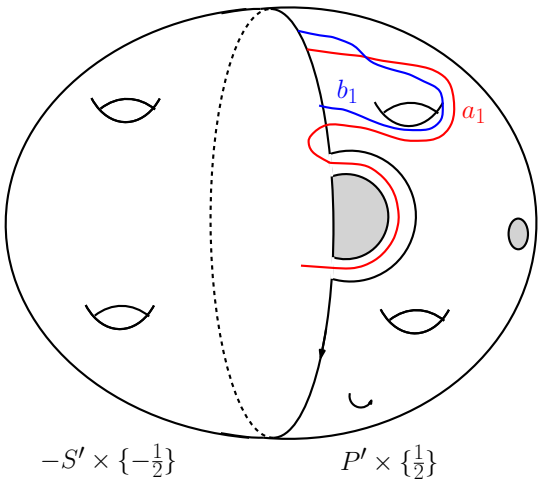

FIGURE 19. Heegaard diagram corresponding to (S', P', h').

Proof of Theorem 5.1. With the identifications above, the proof of Theorem 5.1 is now complete. □

5.2. **Some properties of $\mathcal{L}(L)$.** Next we turn to the proof of the remaining statements.

Proof of Theorem 5.5. Take a standard contact neighborhood $\nu(L)$ of L and stabilize L inside it. Then $L^{\pm}$ has a standard contact neighborhood $\nu(L^{\pm}) \subset \nu(L)$. As it is explained in [16], the contact manifold $(\nu(L) - \nu(L^{\pm}), \xi|_{\nu(L)-\nu(L^{\pm})})$ is a basic slice, i.e., $Y - \nu(L^{\pm})$ is obtained from $Y - \nu(L)$ by a bypass attachment. We can view $Y - \nu(L)$ as the result of a bypass attachment to the boundary of $Y - \nu(L^{\pm})$ *from the back*. As

usual, the two basic slices with the above boundary conditions have opposite relative Euler classes. To figure out which one corresponds to the positive and which one to the negative stabilization we first examine a model case. (For a related discussion see [16].) Suppose that $\mathrm{tb}(L) < 0$ and take a Seifert surface S for L, giving rise to the Seifert surface S^p (resp. S^m) for L^+ (resp. L^-). These surfaces are oriented such that their boundary orientations give the orientations for the knot. Since $\mathrm{tb}(L) < 0$ we can assume that S is in convex position. We have $\mathrm{tb}(L^\pm) = \mathrm{tb}(L) - 1$, thus the dividing curve hits the boundary of the Seifert surface S in $2|\mathrm{tb}(L) - 1|$ points. In the collar neighborhood of the boundary (diffeomorphic to $S^1 \times I$), the dividing curves of S are the line segments $k\frac{2\pi}{2|\mathrm{tb}(L)|} \times I$ where $0 \leq k < 2|\mathrm{tb}(L)|$. Once again, by the negativity of $\mathrm{tb}(L)$ the bypass attachment corresponds to the gluing of an annulus to the boundary of S with dividing curves $k\frac{2\pi}{2|\mathrm{tb}(L)|} \times I$ $(0 \leq k < 2|\mathrm{tb}(L)|)$ and a boundary parallel curve that is disjoint from the others. This boundary parallel curve bounds a domain, cf. Figure 20. The rotation numbers are $\mathrm{rot}(L^\pm) = \mathrm{rot}(L) \pm 1$, thus by the formula $\mathrm{rot}(S) = \chi(S_+) - \chi(S_-)$ we get that the extra domain on S^p (on S^m, resp.) is in the positive (resp. negative) region. Using edge rounding we get that the attaching curve corresponding to the positive (resp. negative) stabilization must end in the positive (resp. negative) region with respect to the orientation of the knot. The left hand side of Figure 21 depicts the arc p (and n, resp.) along which the bypass has to be attached (from the back) to obtain $Y - \nu(L)$.

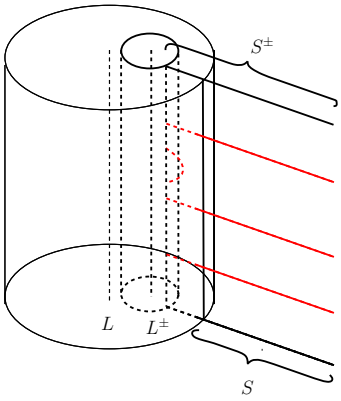

FIGURE 20. Neighborhood of a Legendrian knot and its stabilization.

Both the stabilization and the bypass attachment are local operations, thus the above described phenomenon remains true for any Legendrian knot (without the assumption

$\mathrm{tb}(L) < 0$). The arcs p and n have the same slope, but they end in regions of different sign. Consider the middle diagram of Figure 21 for the general picture for T^2, trivialized by the meridian m and the Thurston–Bennequin framing l.

By Theorem 5.8 the map corresponding to the bypass attachment maps $\mathrm{EH}(L)$ to $\mathrm{EH}(L^{\pm})$. To get $\widehat{\mathcal{L}}(L^{\pm})$ we need to attach another bypass, so that the new dividing curves are meridians, hence this second bypass is attached along the arc c.

In the case of positive stabilization, the manifold $(Y - \nu(L^+), (\xi|_{Y-\nu(L^+)})^c) = (Y - \nu(L), (\xi|_{Y-\nu(L)})^{p^{-1}c})$ is overtwisted. Indeed, performing the positive stabilization first one can indicate both bypasses in one picture, one attached from the back: p^{-1} drawn by dashed line on Figure 21 and c from the front. These curves are parallel, thus the corresponding bypasses ("half overtwisted disks") form an overtwisted disk in $(Y - \nu(L), (\xi|_{Y-\nu(L)})^{p^{-1}c})$. It is known that the sutured invariant of an overtwisted structure vanishes [24, Corollary 4.3.], therefore so does $\widehat{\mathcal{L}}(L^+)$.

In the case of negative stabilization, the contact structure $(T^2 \times I, \xi^{n^{-1}c})$ is universally tight. This can be seen by first passing to $\partial(Y - \nu(L))$ (cf. the right hand side of Figure 21) and then noting that the two bypasses attached there are of the same sign, so they do not induce an overtwisted disk. The union of the two basic slices is minimally twisting, and in this case the range of slopes is $[0, \infty] = [0, 1] \cup [1, \infty]$. Therefore the result is still a basic slice, thus the composition of the two bypass attachments along n and c is equivalent to a single bypass attachment along c. This immediately implies $\widehat{\mathcal{L}}(L) = \widehat{\mathcal{L}}(L^-)$, concluding the proof. □

Next we turn to the proof of the statement concerning the vanishing of the Legendrian invariant in the presence of Giroux torsion. We start by recalling Giroux torsion.

Definition 5.10. The contact structure ξ_n on $T^2 \times [0, 1] = \mathbb{R}/\mathbb{Z} \times \mathbb{R}/\mathbb{Z} \times [0, 1] = \{(x, y, z))\}$ is defined by $\xi_n = \ker(\cos(2\pi nz)dx - \sin(2\pi nz)dy)$. A (not necessarily closed) contact 3–manifold (Y, ξ) has *Giroux torsion* $\tau(Y, \xi) \geq n$ if it contains an embedded submanifold $T^2 \times I$ with the property that $(T^2 \times I, \xi|_{T^2 \times I})$ is contactomorphic to $(T^2 \times [0, 1], \xi_n)$.

Proof of Corollary 5.2. The proof is a simple adaptation of the proof for the closed case given by Ghiggini, Honda, and Van Horn-Morris [20]. As $(Y - \nu(L), \xi_{Y-\nu(L)})$ has positive Giroux torsion, there is a submanifold $T^2 \times I$, such that $\xi|_{T^2 \times I} = \xi_n$ for some $n > 0$. It was shown in [20] that $\mathrm{EH}(T^2 \times I, \xi_n) = 0$.

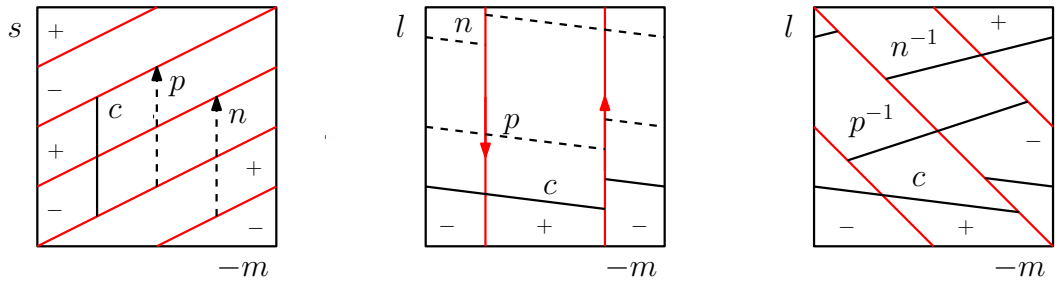

FIGURE 21. Attaching curves for the bypasses corresponding to the stabilizations. The dashed line indicates that the bypass is attached from the back. On the left–hand picture s denotes the Seifert framing of the knot, while on the two right–hand pictures l is given by the contact framing of the Legendrian knot.

The application of Theorem 5.8 for the contact 3–manifold pair $(Y-\nu(L), T^2\times[0,1])$ provides a map

$$\mathrm{SFH}(-(T^2\times I), -\Gamma_{\partial(T^2\times I)}) \to \mathrm{SFH}(-(Y-\nu(L)), -\Gamma_{Y-\nu(L)}))$$

mapping the contact element $\mathrm{EH}(T^2\times I, \xi_n) = 0$ to the contact element $\mathrm{EH}(L) = \mathrm{EH}(Y-\nu(L), \xi|_{Y-\nu(L)})$. This implies that $\mathrm{EH}(L)=0$, hence in the light of Theorem 5.1 we get that $\widehat{\mathcal{L}}(L)=0$, concluding the proof. □

Proof of Theorem 5.7. As in the proof of Theorem 5.1, we attach a bypass along the arc e of Figure 22 and change the dividing curve on the torus boundary to $\Gamma^e_{\partial(Y-\nu(L))}$ of slope -1. There are two choices for such arcs, but again the orientation of L assigns the one depicted on Figure 22.

This bypass attachment gives rise to a map

$$\Phi^e\colon \mathrm{SFH}(-(Y-\nu(L)), -\Gamma_{\partial(Y-\nu(L))}) \to \mathrm{SFH}(-(Y-\nu(L)), -\Gamma^e_{\partial(Y-\nu(L))}).$$

By filling the boundary with a solid torus, the latter homology is identified with $\widehat{\mathrm{HFK}}(-Y_{-1}, L')$. Denote the composition of the above maps by

$$G\colon \mathrm{SFH}(-(Y-\nu(L)), -\Gamma_{\partial(Y-\nu(L))}) \to \widehat{\mathrm{HFK}}(-Y_{-1}, L').$$

We claim that the homomorphism G maps $\mathrm{EH}(L)$ to $\widehat{\mathcal{L}}(L')$. Indeed, consider an open book (S,h) adapted to (Y,ξ,L). The same open book is adapted to (Y_{-1},ξ_{-1},L'),

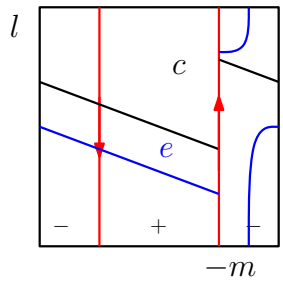

FIGURE 22. Attaching curves for the bypasses on $\partial(Y-\nu(L))$ to obtain dividing curves of slope 1.

with the only difference in the monodromy: the monodromy h' for the latter triple is multiplied by a right–handed Dehn twist along L, cf. [36, page 133]. Using the notations introduced in the beginning of this Section, the map G corresponds to changing the partial open book $(S, P = S - \nu_S(L), h|_P)$ to (S', P', h'') corresponding to the bypass attachment. The image of the half–meridian a_+ under h'' is $h(a^+)$ multiplied by a right–handed Dehn twist along L. Therefore $G(\mathrm{EH}(L)) = \widehat{\mathcal{L}}(L')$.

After attaching the bypass along e, we can apply another bypass attachment along c of Figure 22 to obtain the meridian as dividing curve. We have already seen in the proof of Theorem 5.5 that the composition of these two bypasses is a basic slice, thus we have the commutative diagram

$$\begin{array}{ccc} \mathrm{SFH}(-(Y-\nu(L)), -\Gamma_{\partial(Y-\nu(L))}) & \longrightarrow & \mathrm{SFH}(-(Y-\nu(L)), -\Gamma^e_{\partial(Y-\nu(L))}) = \widehat{\mathrm{HFK}}(-Y_{-1}, L') \\ & \searrow & \downarrow \\ & & \mathrm{SFH}(-(Y-\nu(L)), -m \cup m) = \widehat{\mathrm{HFK}}(-Y, L) \end{array}$$

The maps in the above triangle map the contact invariants as

$$\begin{array}{ccc} \mathrm{EH}(L) & \longrightarrow & \widehat{\mathcal{L}}(L') \\ & \searrow \quad \swarrow & \\ & \widehat{\mathcal{L}}(L) \neq 0 & \end{array}$$

therefore $\widehat{\mathcal{L}}(L')$ does not vanish, concluding the proof. □

6. Transverse simplicity

Multiply pointed Heegaard diagrams turned out to be extremely useful in the case of knots as well, and led to the discovery of a combinatorial version of knot Floer homologies through grid diagrams [32, 31]. This version provided a natural way to define invariants λ_+ and λ_- of Legendrian and θ for transverse knots in the three-sphere [45]. In this section we prove a connected sum formula for these invariants in knot Floer homology:

Theorem 6.1. *Let L_1 and L_2 be (oriented) Legendrian knots. Then there is an isomorphism*

$$\mathrm{HFK}^-(m(L_1)) \otimes_{\mathbb{Z}_2[U]} \mathrm{HFK}^-(m(L_2)) \to \mathrm{HFK}^-(m(L_1\#L_2))$$

which maps $\lambda_+(L_1) \otimes \lambda_+(L_2)$ to $\lambda_+(L_1\#L_2)$. Similar statement holds for the λ_--invariant.

Corollary 6.2. *Let L_1 and L_2 be (oriented) Legendrian knots. Then there is an isomorphism*

$$\widehat{\mathrm{HFK}}(m(L_1)) \otimes_{\mathbb{Z}_2} \widehat{\mathrm{HFK}}(m(L_2)) \to \widehat{\mathrm{HFK}}(m(L_1\#L_2))$$

which maps $\widehat{\lambda}_+(L_1) \otimes \widehat{\lambda}_+(L_2)$ to $\widehat{\lambda}_+(L_1\#L_2)$. Similar statement holds for the $\widehat{\lambda}_-$-invariant. □

Similar results hold for the θ-invariant of transverse knots:

Corollary 6.3. *Let T_1 and T_2 be transverse knots. Then there are isomorphisms*

$$\mathrm{HFK}^-(m(T_1)) \otimes_{\mathbb{Z}_2[U]} \mathrm{HFK}^-(m(T_2)) \to \mathrm{HFK}^-(m(T_1\#T_2))$$

and

$$\widehat{\mathrm{HFK}}(m(T_1)) \otimes_{\mathbb{Z}_2} \widehat{\mathrm{HFK}}(m(T_2)) \to \widehat{\mathrm{HFK}}(m(T_1\#T_2))$$

which map $\theta(T_1) \otimes \theta(T_2)$ to $\theta(T_1\#T_2)$ and $\widehat{\theta}(T_1) \otimes \widehat{\theta}(T_2)$ to $\widehat{\theta}(T_1\#T_2)$, respectively. □

As an application of the above result we prove:

Theorem 6.4. *There exist infinitely many transversely non-simple knots.*

Similar statement follows from the main result of [15], see also [27] and [2]. Even though the statement is about the combinatorial version during the proof we use the

holomorphic interpretation of Heegaard Floer homology. In these versions the Legendrian invariant can be thought of in two different ways, depending on the version of Floer homology we work with. The one introduced in Subsection 4.3 is in the combinatorial Heegaard Floer homology. Once the grid is placed on the torus we get a Heegaard diagram and thus there is a natural identification of the combinatorial Heegaard Floer complex with the holomorphic Heegaard Floer complex [31]. Under this identification the previously defined invariant has a counterpart in the original, holomorphic Heegaard Floer homology. We will use the same notation for both. In the next Subsection we introduce yet another invariant for Legendrian knots.

6.1. **Legendrian invariant on spherical Heegaard diagrams.** A $k\times k$ grid diagram G of a Legendrian knot L of topological type K can also be placed on the 2-sphere in the following way. Let $S^2 = \{(x,y,z) \in \mathbb{R}^3 : \ |(x,y,z)| = 1\}$ and define the circles $\widetilde{\boldsymbol{\alpha}} = \{\widetilde{\alpha}_1, \dots, \widetilde{\alpha}_{k-1}\}$ as the intersection of S^2 with the planes $A_i = \{(x,y,z) \in \mathbb{R}^3 : z = \frac{i}{k} - \frac{1}{2}\}$ $(i = 1, \dots, k-1)$; similarly define $\widetilde{\boldsymbol{\beta}} = \{\widetilde{\beta}_1, \dots, \widetilde{\beta}_{k-1}\}$ as the intersection of S^2 with the planes $B_i = \{(x,y,z) \in \mathbb{R}^3 : \ x = \frac{i}{k} - \frac{1}{2}\}$ $(i = 1, \dots, k-1)$. Call $F = \{(x,y,z) \in \mathbb{R}^3 : \ |(x,y,z)| = 1, y \geq 0\}$ the front hemisphere, and $R = \{(x,y,z) \in \mathbb{R}^3 : \ |(x,y,z)| = 1, y \leq 0\}$ the rear hemisphere. Then there is a grid on both the front and on the rear hemisphere. We place the X's and the O's on the front hemisphere in the way they were placed on the original grid G. After identifying the O's with $\widetilde{\mathbf{w}} = \{\widetilde{w}_1, \dots, \widetilde{w}_k\}$ and the X's with $\widetilde{\mathbf{z}} = \{\widetilde{z}_1, \dots, \widetilde{z}_k\}$ this defines a Heegaard diagram $(S^2, \widetilde{\boldsymbol{\alpha}}, \widetilde{\boldsymbol{\beta}}, \widetilde{\mathbf{w}}, \widetilde{\mathbf{z}})$ with multiple basepoints for (S^3, K). A spherical grid diagram for the trefoil knot is shown by Figure 24.

Let L be a Legendrian knot in S^3. To define the spherical Legendrian invariant $\lambda_+^S(L)$ we will use a grid diagram that have an X in its upper right corner. This can always be arranged by cyclic permutation, but in the following we will need a slightly stronger property:

Lemma 6.5. *For any Legendrian knot there exists a grid diagram representing it which contains an X in its upper right corner and an O in its lower left corner.*

Proof. Consider any grid diagram describing the Legendrian knot L. As it is illustrated on Figure 23, we can obtain a suitable diagram as follows. First do a stabilization of type $X:NE$ and then do a stabilization of type $O:NE$ on the newly obtained O. Lastly, by cyclic permutation we can place the lower X introduced in the first stabilization to

the upper right corner of the diagram. Notice that the O on the upper right of this X will be automatically placed to the lower left corner. According to Proposition 4.1 the Legendrian type of the knot is fixed under these moves, thus the statement follows.

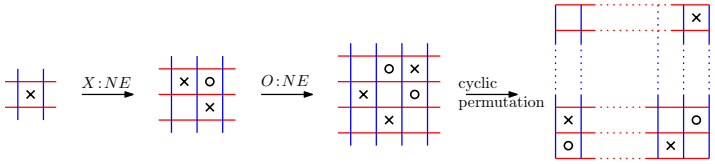

FIGURE 23. Grid moves

□

Suppose, that G is a grid diagram having an X in its upper right corner. Form a spherical grid diagram as above. Define $\mathbf{x}^S_+(L)$ as the generator of $CFK^-(S^2, \widetilde{\boldsymbol{\alpha}}, \widetilde{\boldsymbol{\beta}}, \widetilde{\mathbf{w}}, \widetilde{\mathbf{z}})$ consisting of those intersection points on the front hemisphere that occupy the upper right corner of each region marked with an X. Note that the X in the upper right corner has no such corner. On Figure 24 the element $\mathbf{x}^S_+$ is indicated for the trefoil knot. Similarly to the toroidal case we have:

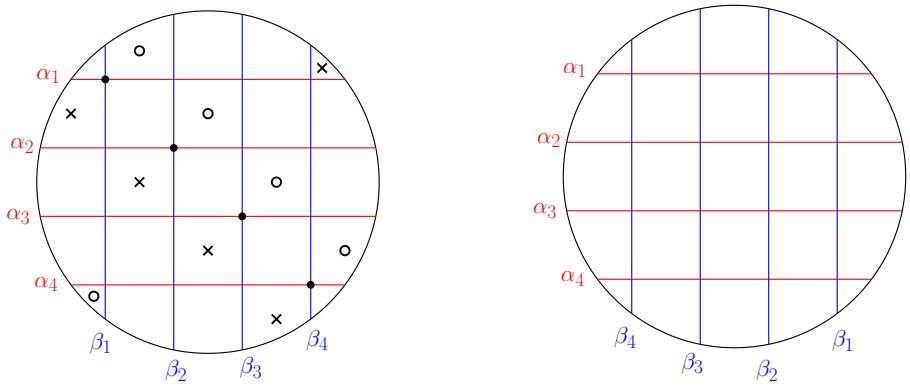

front hemisphere rear hemisphere

FIGURE 24. Spherical grid diagram for the trefoil knot

Lemma 6.6. *The element $\mathbf{x}^S_+(L)$ is a cycle in $(S^2, \widetilde{\boldsymbol{\alpha}}, \widetilde{\boldsymbol{\beta}}, \widetilde{\mathbf{w}}, \widetilde{\mathbf{z}})$.*

Proof. We will show that for any $\mathbf{y}$ there is no positive disc $\psi \in \pi_2(\mathbf{x}^S_+, \mathbf{y})$ with $\mu(\psi) = 1$. As the diagram $CFK^-(S^2, \widetilde{\boldsymbol{\alpha}}, \widetilde{\boldsymbol{\beta}}, \widetilde{\mathbf{w}}, \widetilde{\mathbf{z}})$ is "nice" in the sense of [48] the elements $\mathbf{x}^S_+$ and

$\mathbf{y}$ differ either in one coordinate and $\mathcal{D}(\psi)$ is a bigon or they differ in two coordinates and $\mathcal{D}(\psi)$ is a rectangle. In any case, $\mathcal{D}(\psi)$ contains an X which means it is not counted in the boundary map. □

The homology class of $\mathbf{x}^S_+$, denoted by $\lambda^S_+(G)$, turns out to be an invariant of L (i.e. it is independent of the choice of the grid diagram, and the way it is placed on the sphere). This can be proved directly through grid moves, but instead we show:

Theorem 6.7. *Consider a grid diagram for the Legendrian knot L in S^3 having an X in its upper right corner. Then there is a filtered quasi-isomorphism $\psi : CFK^-(T^2, \boldsymbol{\alpha}, \boldsymbol{\beta}, \mathbf{w}, \mathbf{z}) \to CFK^-(S^2, \widetilde{\boldsymbol{\alpha}}, \widetilde{\boldsymbol{\beta}}, \widetilde{\mathbf{w}}, \widetilde{\mathbf{z}})$ of the corresponding toroidal and spherical Heegaard diagrams which maps $\mathbf{x}_+(L)$ to $\mathbf{x}^S_+(L)$.*

In the proof we will need the notion of Heegaard triples, which we will briefly describe here. (For a complete discussion see [41].) Consider a pointed Heegaard triple $(\Sigma, \boldsymbol{\alpha}, \boldsymbol{\beta}, \boldsymbol{\gamma}, \mathbf{z})$. The pairs $(\Sigma, \boldsymbol{\alpha}, \boldsymbol{\beta}, \mathbf{z})$, $(\Sigma, \boldsymbol{\beta}, \boldsymbol{\gamma}, \mathbf{z})$ and $(\Sigma, \boldsymbol{\alpha}, \boldsymbol{\gamma}, \mathbf{z})$ define the three-manifolds $Y_{\alpha\beta}$, $Y_{\gamma\beta}$ and $Y_{\alpha\gamma}$, respectively. There is a map from $\mathrm{CF}^-(\Sigma, \boldsymbol{\alpha}, \boldsymbol{\beta}, \mathbf{z}) \otimes \mathrm{CF}^-(\Sigma, \boldsymbol{\beta}, \boldsymbol{\gamma}, \mathbf{z})$ to $\mathrm{CF}^-(\Sigma, \boldsymbol{\alpha}, \boldsymbol{\gamma}, \mathbf{z})$ given on a generator $\mathbf{x} \otimes \mathbf{y}$ by

$$\sum_{\mathbf{v} \in \mathbb{T}_\alpha \cap \mathbb{T}_\gamma} \sum_{\substack{u \in \pi_2(\mathbf{x}, \mathbf{y}, \mathbf{v}) \\ n_{\mathbf{z}}(u) = 0 \\ \mu(u) = 0}} |\mathcal{M}(u)| \mathbf{v}$$

where $\pi_2(\mathbf{x}, \mathbf{y}, \mathbf{v})$ is the set of homotopy classes of triangles connecting $\mathbf{x}$, $\mathbf{y}$ to $\mathbf{v}$; maps from a triangle to $\mathrm{Sym}^{g+k-1}(\Sigma)$ sending the edges of the triangle to $\mathbb{T}_\alpha$,$\mathbb{T}_\beta$ and $\mathbb{T}_\gamma$, $\mathcal{M}(u)$ is the moduli space of pseudo-holomorphic representatives of the homotopy class u. This gives a well-defined map on the homologies HF^-. When $\boldsymbol{\gamma}$ can be obtained from $\boldsymbol{\beta}$ by Heegaard moves then the manifold $Y_{\beta\gamma}$ is $\#^g S^1 \times S^2$ and $\mathrm{HF}^-(\#^g S^1 \times S^2)$ is a free $\mathbb{Z}_2[U]$-module generated by 2^g-elements. Denote its top-generator by $\Theta^-_{\beta\gamma}$. The same definition gives a map on the filtered chain complexes CFK^-. The map $CFK^-(Y_{\alpha\beta}) \to CFK^-(Y_{\alpha\gamma})$ sending $\mathbf{x}$ to the image of $\mathbf{x} \otimes \Theta^-_{\beta\gamma}$ defines a quasi-isomorphism of the chain complexes.

Proof of theorem 6.7. From a toroidal grid diagram one can obtain a spherical one by first sliding every β-curve over β_1 to obtain $\boldsymbol{\beta}'$ and sliding every α-curve over α_1 to obtain $\boldsymbol{\alpha}'$, and then destabilize the diagram at α_1 and β_1. Thus we will construct the

quasi-isomorphism by the composition $\psi = \psi_{\text{destab}} \circ \psi_\alpha \circ \psi_\beta$, where

$$\psi_\beta = \sum_{\mathbf{y} \in \mathbb{T}_\alpha \cap \mathbb{T}_{\beta'}} \sum_{\substack{u \in \pi_2(\mathbf{x}_+(L), \Theta^-, \mathbf{y}) \\ n_{\mathbf{z}}(u)=0 \\ \mu(u)=0}} |\mathcal{M}(u)|\mathbf{y}$$

where $\Theta^- \in \mathbb{T}_\beta \cap \mathbb{T}_{\beta'}$ is the top generator of $\mathrm{HF}^-(T^2, \boldsymbol{\beta}, \boldsymbol{\beta'}, \mathbf{z}) = \mathrm{HF}^-(S^1 \times S^2)$ and ψ_α defined similarly. Note that in the case of the sliding there is also a "closest point" map denoted by $'$ for the sliding of the $\boldsymbol{\beta}$–curves and by $''$ for the sliding of the $\boldsymbol{\alpha}$–curves. We claim:

Lemma 6.8. $\psi_\beta(\mathbf{x}_+) = \mathbf{x}'_+$.

Lemma 6.9. $\psi_\alpha(\mathbf{x}'_+) = (\mathbf{x}'_+)''$.

Here we just include the proof of Lemma 6.8; Lemma 6.9 follows similarly.

Proof of Lemma 6.8. Figure 25 shows a weakly admissible diagram for the slides of the $\boldsymbol{\beta}$–curves.

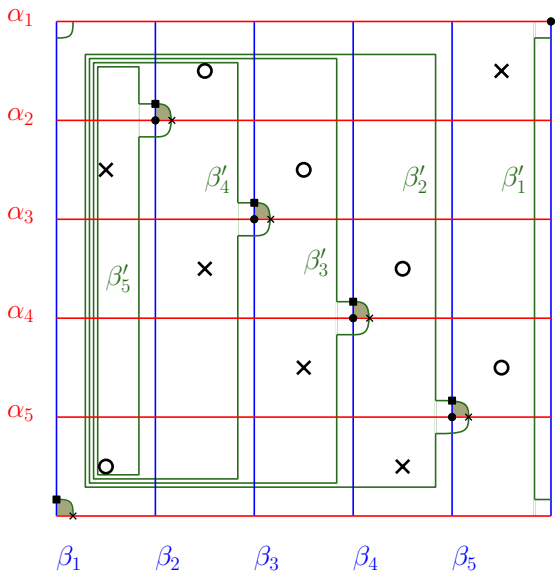

FIGURE 25. Handleslides

Claim 1. *The Heegaard triple* $(T^2, \boldsymbol{\alpha}, \boldsymbol{\beta}, \boldsymbol{\beta'}, \mathbf{z})$ *of Figure 25 is weakly admissible.*

Proof. Let $\mathcal{P}_{\beta_i\beta'_i\beta_1}$ $(i>1)$ denote the domain bounded by β_i, β'_i and β_1 and containing no basepoint. Similarly $\mathcal{P}_{\beta_1\beta'_1}$ denotes the domain bounded by β_1 and β'_1 and containing no basepoint. These domains form a basis for the periodic domains of $(T^2,\boldsymbol{\beta},\boldsymbol{\beta'},\mathbf{z})$ and as all have domains with both positive and negative coefficients we can see that $(T^2,\boldsymbol{\beta},\boldsymbol{\beta'},\mathbf{z})$ is weakly admissible. Consider a triply periodic domain $\mathcal{P}$. If there is no α-curve in its boundary, then it is a periodic domain of $(T^2,\boldsymbol{\beta},\boldsymbol{\beta'},\mathbf{z})$, and by the previous observation we are done. So $\mathcal{P}$ must contain an α-curve in its boundary. To ensure it does not contain an X, there must be some vertical curve, either from β or β', in the boundary. At the intersection point of the horizontal and vertical lines the domain must change sign, concluding the argument. □

The grey area in Figure 25 indicates a domain of a canonical triangle u_0 connecting $\mathbf{x}_+(L)$,Θ^- and $\mathbf{x}'_+(L)$; by the Riemann mapping theorem there is exactly one map with that domain. We claim that this is the only map that is encountered in ψ_β. For this, let $u\in\pi_2(\mathbf{x}_+(L),\Theta^-,\mathbf{y})$ be a holomorphic triangle with $\mu(u)=0$ and $n_{\mathbf{z}}(u)=0$.

Claim 2. *There exists a periodic domain $\mathcal{P}_{\beta\beta'}$ of $(T^2,\boldsymbol{\beta},\boldsymbol{\beta'},\mathbf{z})$ such that $\partial(\mathcal{D}(u)-\mathcal{D}(u_0)-\mathcal{P}_{\beta\beta'})|_{\boldsymbol{\beta}}=\emptyset$. Thus $(\mathcal{D}(u)-\mathcal{D}(u_0)-\mathcal{P}_{\beta\beta'})$ is a domain in $(T^2,\boldsymbol{\alpha},\boldsymbol{\beta'},\mathbf{z})$, representing an element v in $\pi_2(\mathbf{x}'_+,\mathbf{y})$ with Maslov index $\mu(v)=\mu(u)-\mu(u_0)-\mu(\mathcal{P}_{\beta\beta'})=0$.*

Proof. As $n_{\mathbf{z}}(u)=0$ and $\mathbf{x}'_+(L)$ is in the upper right corner of the X's, the domain of any triangle must contain $\mathcal{D}(u_0)$. Consequently $\partial\mathcal{D}(u)|_{\beta_i}$ is an arc containing the small part $\overline{\mathcal{D}(u_0)}\cap\beta_i$ and some copies of the whole β_i. By subtracting $\mathcal{D}(u_0)$ and sufficiently many copies of the periodic domains $\mathcal{P}_{\beta_i\beta'_i\beta_1}$ we obtain a domain with no boundary component on β_i. Doing the same process for every $i>1$ and then by subtracting some $\mathcal{P}_{\beta_1\beta'_1}$ we can eliminate every β_i from the boundary. □

Claim 3. *There is no positive disc in $\pi_2(\mathbf{x}'_+,\mathbf{y})$.*

Proof. This follows similarly to Lemma 6.6. □

Claim 4. *None of the regions of $(T^2,\boldsymbol{\alpha},\boldsymbol{\beta'},\mathbf{z})$ can be covered completely with the periodic domains of $(T^2,\boldsymbol{\beta},\boldsymbol{\beta'},\mathbf{z})$ and $\mathcal{D}(u_0)$.*

Proof. The periodic domains are the linear combinations of $\{\mathcal{P}_{\beta_i,\beta'_i,\beta_1}\}_{i=2}^k\cup\{\mathcal{P}_{\beta_1,\beta'_1},\}$, and those cannot cover the domains of $(T^2,\boldsymbol{\alpha},\boldsymbol{\beta'},\mathbf{z})$. □

Putting these together, we have that $\mathcal{D}(u) - \mathcal{D}(u_0) - \mathcal{P}_{\beta\beta'}$ has a negative coefficient, which gives a negative coefficient in $\mathcal{D}(u)$ as well, contradicting the fact that u was holomorphic. This proves Lemma 6.8. □

Note that by assuming that there is an X in the upper right corner of the grid diagram we assured that the intersection point $\mathbf{x}_+$ contains $\alpha_1 \cap \beta_1$, and that point remained unchanged during the whole process. Thus by destabilizing at α_1 and β_1 we get Theorem 6.7. □

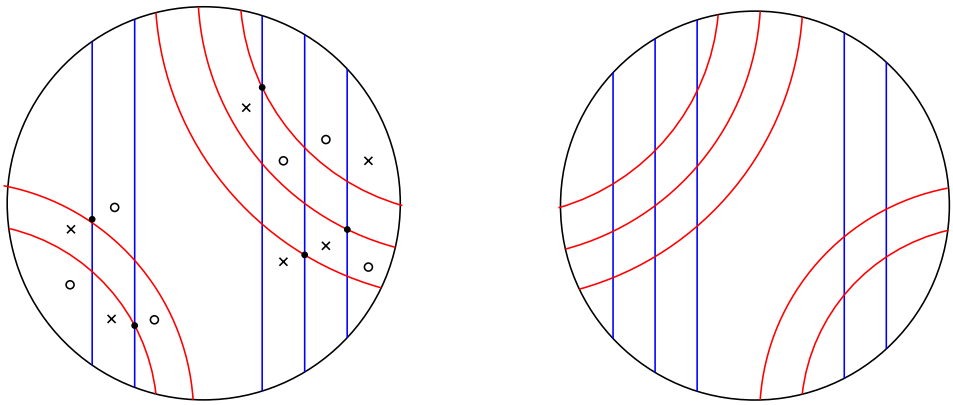

front hemisphere rear hemisphere

FIGURE 26. Connected Sum

Proof of Theorem 6.1. Consider two Legendrian knots L_1 and L_2 of topological types K_1 and K_2. Note that once we obtain the result for λ_+^S we are done. Indeed, passing from the toroidal diagram to the spherical one, the invariants $\lambda_+(L_1)$ and $\lambda_+(L_2)$ are mapped to $\lambda_+^S(L_1)$ and $\lambda_+^S(L_2)$, respectively. Knowing that $\lambda_+^S(L_1) \otimes \lambda_+^S(L_2)$ is mapped to $\lambda_+^S(L_1 \# L_2)$ and passing back to the toroidal diagram, there is an isomorphism that maps this to $\lambda_+(L_1 \# L_2)$. So the combination of these arguments prove Theorem 6.1.

Consider the grid diagrams G_1 and G_2 corresponding to L_1 and L_2 admitting the conditions of Lemma 6.5. These grids define the spherical grid diagrams $(S^2, \boldsymbol{\alpha}_1, \boldsymbol{\beta}_1, \mathbf{w}_1, \mathbf{z}_1)$ and $(S^2, \boldsymbol{\alpha}_2, \boldsymbol{\beta}_2, \mathbf{w}_2, \mathbf{z}_2)$. Let $z \in \mathbf{z}_1$, $w \in \mathbf{w}_2$ be the basepoints corresponding to the X in the upper right corner of the first diagram and the O in the lower left corner of the second diagram. Form the connected sum of $(S^2, \boldsymbol{\alpha}_1, \boldsymbol{\beta}_1, \mathbf{w}_1, \mathbf{z}_1)$ and $(S^2, \boldsymbol{\alpha}_2, \boldsymbol{\beta}_2, \mathbf{w}_2, \mathbf{z}_2)$ at the regions containing z and w to obtain a Heegaard diagram with multiple basepoints $(S^2, \boldsymbol{\alpha}_1 \cup \boldsymbol{\alpha}_2, \boldsymbol{\beta}_1 \cup \boldsymbol{\beta}_2, \mathbf{w}_1 \cup (\mathbf{w}_2 - \{w\}), (\mathbf{z}_1 - \{z\} \cup \mathbf{z}_2))$ of $(S^3, L_1 \# L_2)$. By 2.10

the map

$$\psi_{\text{connsum}}: \quad \mathrm{HFK}^-(S^2, \boldsymbol{\alpha}_1, \boldsymbol{\beta}_1, \mathbf{w}_1, \mathbf{z}_1) \otimes \mathrm{HFK}^-(S^2, \boldsymbol{\alpha}_2, \boldsymbol{\beta}_2, \mathbf{w}_2, \mathbf{z}_2) \to$$
$$\mathrm{HFK}^-(S^2, \boldsymbol{\alpha}_1 \cup \boldsymbol{\alpha}_2, \boldsymbol{\beta}_1 \cup \boldsymbol{\beta}_2, \mathbf{w}_1 \cup (\mathbf{w}_2 - \{w\}), (\mathbf{z}_1 - \{z\}) \cup \mathbf{z}_2)$$

defined on the generators as $\mathbf{x}_1 \otimes \mathbf{x}_2 \mapsto (\mathbf{x}_1, \mathbf{x}_2)$ is an isomorphism. Thus the image of $\lambda^S_+(L_1) \otimes \lambda^S_+(L_2)$ is $(\lambda^S_+(L_1), \lambda^S_+(L_2))$.

Figure 26 shows the resulting Heegaard diagram. From this diagram of the connected sum one can easily obtain a spherical grid diagram by isotoping every curve in $\boldsymbol{\alpha}_1$ to intersect the curves in $\boldsymbol{\beta}_2$ and every curve in $\boldsymbol{\alpha}_2$ to intersect the curves in $\boldsymbol{\beta}_1$ as shown on Figure 27. Indeed, the resulting diagram is a grid obtained by patching G_1 and G_2 together in the upper right X of G_1 and the lower left O of G_2 and deleting the X and O at issue. Now by connecting the X in the lower row of G_2 to the O in the upper row of G_1, and proceeding similarly in the columns we get that the grid corresponds to the front projection of $L_1 \# L_2$. Again, a quasi-isomorphism ψ_{isot} is given with the help of holomorphic triangles. A similar argument as in the proof of Lemma 6.8 shows that under the isomorphism induced by ψ_{isot} on the homologies, the element $(\lambda^S_+(L_1), \lambda^S_+(L_2))$ is mapped to $\lambda^S_+(L_1 \# L_2)$.

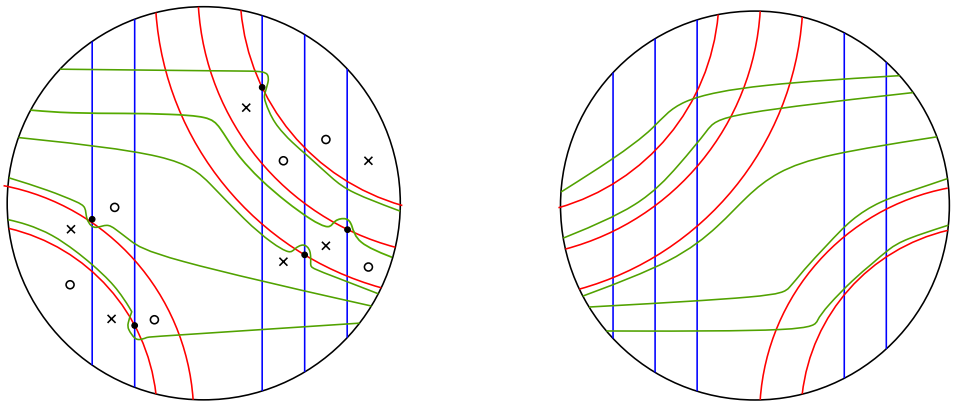

front hemisphere rear hemisphere

FIGURE 27. Isotoping to obtain a grid diagram

□

6.2. **Proof of Theorem 6.4.** One way of distinguishing transverse knots in a given knot type is to prove that their $\widehat{\theta}$-invariants are different. This, however, cannot be

done straightforwardly as the vector space $\widehat{\mathrm{HFK}}$ does not canonically correspond to a knot. So in order to prove that two elements are different, we have to show that there is no isomorphism of $\widehat{\mathrm{HFK}}$ carrying one to the other. More explicitly, it is enough to see that there is no such isomorphism induced by a sequence of Heegaard moves. For instance, if we show that one element is 0, while the other is not, we can be certain that they are different. This is used in the proof of Theorem 6.4.

Proof of Theorem 6.4. Ng, Ozsváth and Thurston [35] showed that the knot type 10_{132} contains transversely non-isotopic representatives L_1 and L_2 with equal self-linking number. They proved that $\widehat{\theta}(L_1)$ is zero in $\widehat{\mathrm{HFK}}(m(10_{132}))$ while $\widehat{\theta}(L_2)$ is not. In the following we will prove that the knot types $\#^n 10_{132}$ are transversely non-simple. By the uniqueness of prime decomposition of knots [3], these are indeed different knot types. Thus this list provides infinitely many examples of transversely non-simple knots. The two transversely non isotopic representatives of $\#^n 10_{132}$ are $\#^n L_2$ and $L_1\#(\#^{n-1}L_2)$. Using the formula $\mathrm{sl}(L_1'\#L_2') = \mathrm{sl}(L_1') + \mathrm{sl}(L_2') + 1$ for the self-linking numbers we have $\mathrm{sl}(\#^n L_2) = n\mathrm{sl}(L_2) + (n-1) = \mathrm{sl}(L_1) + (n-1)\mathrm{sl}(L_2) + (n-1) = \mathrm{sl}(L_1\#(\#^{n-1}L_2))$. We use Corollary 6.2 to distinguish the transverse isotopy types of $\#^n L_2$ and $L_1\#(\#^{n-1}L_2)$. There is an isomorphism from $\widehat{\mathrm{HFK}}(m(10_{132})) \otimes \widehat{\mathrm{HFK}}(\#^{n-1}m(10_{132}))$ to $\widehat{\mathrm{HFK}}(\#^n m(10_{132}))$ mapping $\widehat{\theta}(L_1)\otimes\widehat{\theta}(\#^{n-1}L_2)) = 0$ to $\widehat{\theta}(L_1\#(\#^{n-1}L_2))$, thus it is zero. Similarly, there is an isomorphism mapping $\widehat{\theta}(L_2) \otimes \widehat{\theta}(\#^{n-1}L_2)) \neq 0$ to $\widehat{\theta}(L_2\#(\#^{n-1}L_2))$, thus by induction on n it does not vanish.

□

References

[1] V. I. Arnold. First steps in symplectic topology. *Russian Math. Surveys*, 41:1–21, 1986.

[2] J. S. Birman and W. M. Menasco. Stabilization in the braid groups II. Transversal simplicity of knots. *Geometry & Topology*, 10:1425–1452, 2006. math.GT/0310280.

[3] G. Burde and H. Zieschang. *Knots*, volume 5. Walter de Gruyter, New York, 2003.

[4] Y. Chekanov. Differential algebra of Legendrian links. *Invent. Math.*, 150(3):441–483, 2002.

[5] Y. Eliashberg. Classification of overtwisted contact structures on 3-manifolds. *Invent. Math.*, 98:623–637, 1989.

[6] Y. Eliashberg. Contact 3–manifolds twenty years since J. Martinet's work. *Ann. Inst. Fourier*, 42:165–192, 1992.

[7] Y. Eliashberg. The classification of tight contact structures on the 3–torus. *Comm. in Anal. and Geom.*, 5:207–255, 1997.

[8] Y. Eliashberg. Invariants in contact topology. *Proceedings of the International Congress of Mathematicians Doc. Math.*, II:327–338, 1998.

[9] Y. Eliashberg and M. Fraser. Classification of topologically trivial Legendrian knots. In *Geometry topology and dynamics CRM Proc. Lecture Notes*, volume 15, pages 17–51. Amer. Math. Soc., 1998. arXiv:0801.2553.

[10] T. Etgü and B. Ozbagci. Partial open book decompositions and the contact class in sutured Floer homology. 2007. arXiv:0711.0880.

[11] T. Etgü and B. Ozbagci. Relative Giroux correspondence. 2007. arXiv:0802.0810.

[12] J. B. Etnyre. Private communication.

[13] J. B. Etnyre. Introductory lectures on contact geometry. *Proc. Sympos. Pure Math.*, 71:81–107, 2003. arXiv:math/0111118v2.

[14] J. B. Etnyre. Legendrian and transversal knots. In *Handbook of knot theory*, pages 105–185. Elsevier B. V., 2005.

[15] J. B. Etnyre and K. Honda. Cabling and transverse simplicity. *Ann. of Math.*, 162(3):1305–1333, 2001. arXiv:math/0306330v2.

[16] J. B. Etnyre and K. Honda. Knots and contact geometry. I. Torus knots and the figure eight knot. *J. Symplectic Geom.*, 1(1):63–120, 2001. arXiv:math/0006112v1.

[17] A. Floer. Morse theory for Lagrangian intersections. *J. Differential Geometry*, 28:513–547, 1988.

[18] A. Floer and H. Hofer. Coherent orientations for periodic orbit problems in symplectic geometry. *Math. Z.*, 212:13–38, 1993.

[19] P. Ghiggini and K. Honda. Giroux torsion and twisted coefficients. arXiv:0804.1568.

[20] P. Ghiggini, K. Honda, and J. Van Horn-Morris. The vanishing of the contact invariant in the presence of torsion. arXiv:0706.1602v2.

[21] E. Giroux. Convexité en topologie de contact. *Comment. Math. Helv.*, 66:637–677, 1991.

[22] E. Giroux. Structures de contact sur les variétés fibrées en cercles dune surface. *Comment. Math. Helv.*, 76:218–262, 2001.

[23] K. Honda. On the classification of tight contact structures I. *Geometry & Topology*, 4:309–368, 2000. arXiv:math/9910127.

[24] K. Honda, W. Kazez, and G. Matić. The contact invariant in sutured Floer Homology. 2007. arXiv:0705.2828v2.

[25] K. Honda, W. Kazez, and G. Matić. Contact structures, sutured Floer homology, and TQFT. 2008. arXiv:0807.2431v1.

[26] A. Juhász. Holomorphic discs and sutured manifolds. *Algebraic & Geometric Topology*, 6:1429–1457, 2006. arXiv:math/0601443v2.

[27] K. Kawamuro. Connect sum and transversely non simple knots. 2008. math/08022585.

[28] Rob Kirby. Problems in low-dimensional topology. In *Proceedings of Georgia Topology Conference, Part 2*, pages 35–473. Press, 1996.

[29] P. Kronheimer and T. Mrowka. Witten's conjecture and property P. *Geometry & Topology*, 8:295–310, 2004. arXiv:math/0311489v5.

[30] P. Lisca, P. Ozsváth, A. Stipsicz, and Z. Szabó. Heegaard Floer invariants of Legendrian knots in contact 3-manifolds. 2008. arXiv:0802.0628v1.

[31] C. Manolescu, P. Ozsváth, and S. Sarkar. A combinatorial description of knot Floer homology. math/0607691.

[32] C. Manolescu, P. Ozsváth, Z. Szabó, and D. Thurston. On combinatorial link Floer homology. math/0610559.

[33] J. Martinet. *Formes de contact sur les variétés de dimension 3*, volume 209, pages 295–310. Springer, Berlin, 1971.

[34] J. Milnor. *Morse Theory*. Princeton Univ. Press, 1963.

[35] L. Ng, P. Ozsváth, and D. Thurston. Transverse knots distinguished by knot Floer homology. *Algebraic &. Geometric Topology*, 5:1637–1653, 2004. math/0703446.

[36] B. Ozbagci and A. Stipsicz. *Surgery on Contact 3-Manifolds and Stein Surfaces*, volume 13 of *Bolyai Society Mathematical Studies*. Springer-Verlag, Berlin, ninth dover printing, tenth gpo printing edition, 2004.

[37] P. Ozsváth and A. Stipsicz. Contact surgeries and the transverse invariant in knot Floer homology. arXiv:0803.1252.

[38] P. Ozsváth and Z. Szabó. Holomorphic disks and genus bounds. *Geometry & Topology*, 8, 2004. arXiv:math/0311496v3.

[39] P. Ozsváth and Z. Szabó. Holomorphic disks and knot invariants. *Adv. Math.*, 186(1):58–116, 2004.

[40] P. Ozsváth and Z. Szabó. Holomorphic disks and three-manifold invariants: properties and applications. *Ann. of Math.*, 159(2):1159–1245, 2004. arXiv:math/0105202v4.

[41] P. Ozsváth and Z. Szabó. Holomorphic disks and topological invariants for closed three-manifolds. *Ann. of Math. (2)*, 159(3):1027–1158, 2004.

[42] P. Ozsváth and Z. Szabó. Heegaard Floer homology and contact structures. *Duke Math. J.*, 129(1):39–61, 2005. arXiv:math/0210127v1.

[43] P. Ozsváth and Z. Szabó. Holomorphic triangles and invariants for smooth four-manifolds. *Advances in Mathematics*, 202(2):326–400, 2006. arXiv:math/0110169v2.

[44] P. Ozsváth and Z. Szabó. Holomorphic discs, link invariants, and the multi-variable Alexander polynomial. *Algebraic & Geometric Topology*, 8:615–692, 2008. math/0512286.

[45] P. Ozsváth, Z. Szabó, and D. Thurston. Legendrian knots, transverse knots and combinatorial Floer homology. arXiv:math/0611841v2.

[46] J. A. Rasmussen. *Floer homology and knot complements*. Phd thesis, Harvard University, 2003. math/0607691.

[47] K. Reidemeister. Zur dreidimensionalen topologie. *Abh. Math. Sem. Univ. Hamburg*, 9, 1936.

[48] S. Sarkar and J. Wang. An algorithm for computing some Heegaard Floer homologies. arXiv:math/0607777.

[49] J. Singer. Three-dimensional manifolds and their heegaard-diagrams. *Trans. Amer. Math. Soc.*, 35, 1933.

[50] I. Torisu. Convex contact structures and fibered links in 3-manifolds. *Internat. Math. Res. Notices*, 9:441–454, 2000.

[51] D. S. Vela-Vick. On the transverse invariant for bindings of open books. arXiv:0806.1729.